

BACHELOR PHYSICS AND ASTRONOMY

 UNIVERSITY OF AMSTERDAM

VU  **VRIJE
UNIVERSITEIT
AMSTERDAM**

Determining suitable models for
C. elegans locomotion by
evaluating Lyapunov exponents

Nardi Lam,
10453555

4 July 2018

Supervisor: Greg Stephens

Signed by: Greg Stephens, Edan Lerner

Abstract

Building on the discovery that *C. elegans* locomotive dynamics are governed by an attractor in a 6-D phase space [1], models that emulate these dynamics are researched. The dynamics are characterised by the dynamically invariant quantities known as the Lyapunov exponents (LEs), which for *C. elegans* form a symmetric Lyapunov spectrum. Two types of models are investigated in detail: a pair of coupled Nosé-Hoover (N-H) oscillators, and a pendulum driven by a periodic force.

By comparing the values of the LEs for these models to those obtained from the *C. elegans* dynamics, it is shown that a single driven pendulum cannot produce a similarly symmetric spectrum and has to be extended in some way. Coupling the N-H oscillators also breaks the symmetry of the LEs, however, different configurations show a wide range of behavior which indicates they might be useful if coupled differently.

Populaire samenvatting

In de natuurkunde worden over het algemeen niet-levende objecten onderzocht, zoals een projectiel of een slinger. Deze vertonen simpel gedrag: ze schieten door de ruimte of ze zwaaien heen en weer. Het is echter veel ingewikkelder om het gedrag van bijvoorbeeld een dier te beschrijven. Sommige kleine organismen zijn door biologen uitvoerig onderzocht. Een voorbeeld daarvan is een millimeter-groot wormpje genaamd *C. elegans*, waarvan vrijwel het hele lichaam en brein in kaart is gebracht. Dit wormpje doet niet veel meer dan rondkruipen op zoek naar eten. Desondanks is het lastig om te omschrijven hóé het precies kruipt. Daarentegen kunnen natuurkundigen wel heel precies bepalen hoe bijvoorbeeld een ruimteschip op een komeet kan landen. De vraag is: kan een natuurkundige aanpak ook bij dit soort levende wezens leiden tot meer begrip van hoe ze werken?

Om te begrijpen wat die natuurkundige aanpak is, zal ik een paar begrippen uitleggen. In het algemeen houdt de natuurkunde zich bezig met het bestuderen van **systemen**. Dit zijn dingen in de natuur waarvan je bepaalde **eigenschappen** kan meten. Meestal blijven deze eigenschappen niet hetzelfde, maar veranderen ze in de loop der tijd. In dat geval hebben we het over een **dynamisch systeem**. Denk aan een auto die ergens recht vooruit rijdt: deze bevindt zich op een bepaalde locatie (*lengte-* en *breedtegraad*), en rijdt met een bepaalde *snelheid* in een bepaalde *richting*. Deze rijdende auto kunnen we beschrijven met in totaal 4 eigenschappen (waarvan twee voor de locatie), ook wel het aantal **dimensies** genoemd.

Het doel is uiteindelijk om te proberen om de beweging van *C. elegans* ook te beschrijven als een dynamisch systeem. Dat is echter nog een heel eind weg. Wel is het mogelijk om al te kijken naar een aantal algemene aspecten van dit (onbekende) wormsysteem. Zo is ontdekt dat dit systeem met slechts 6 dimensies uit de voeten kan.

Daarnaast zijn bepaalde karakteristieke getallen voor het wormsysteem geschat, de zogenaamde **Lyapunov-exponenten**. Deze getallen geven aan hoe veel variatie er in de dynamiek van een

systeem zit. In het geval van de auto is dit als volgt te bepalen: stel we nemen twee auto's, en plaatsen deze op twee locaties vlakbij elkaar. Ook zetten we ze in bijna dezelfde richting, maar met een kleine afwijking. Nu laten we ze allebei rijden, maar één auto net iets sneller dan de ander.

Als we ze na een lange tijd laten stoppen met rijden, wat is er dan gebeurd? De auto's reden in verschillende richtingen, dus hoe langer we ze laten rijden, hoe meer de locaties uit elkaar komen te liggen. Dat betekent dat bij de twee getallen die bij de locatie horen voor beide een *positieve* (groter dan nul) Lyapunov-exponent hoort. De andere eigenschappen, snelheid en richting, zijn echter niet veranderd en verschillen nog steeds maar een klein beetje voor de twee auto's. Dat betekent dat bij deze twee eigenschappen Lyapunov-exponenten *gelijk aan nul* horen. Het rijdende auto-systeem heeft dus 4 Lyapunov-exponenten: twee positief en twee gelijk aan nul.

Voor *C. elegans* is bekend dat het 6 van deze exponenten heeft: twee positief, één gelijk aan nul en drie negatief. Daarom heb ik twee systemen onderzocht die mogelijk ook zulke exponenten hebben. Het eerste systeem bestaat uit twee aan elkaar gekoppelde **Nosé-Hoover oscillatoren**: een simpel soort slingers die op constante temperatuur gehouden worden. Het tweede systeem is een normale slinger die door een Van der Pol-oscillator (ook een soort aangepaste slinger) wordt aangedreven. Deze systemen zijn uitgekozen omdat ze gebaseerd zijn op bekende, slinger-achtige systemen en daarom niet te lastig zijn om mee te rekenen, maar wel ingewikkeld genoeg zijn om bijzonder soort gedrag te kunnen vertonen.

Ik heb simulaties van deze systemen gedaan, om zo de exponenten te berekenen. Hieruit blijkt dat het eerste systeem nogal ingewikkeld in elkaar zit en daardoor veel variatie laat zien in zijn gedrag. Om duidelijker te bepalen of dit systeem op *C. elegans* kan lijken moet het daarom verder beperkt worden. Het tweede systeem is echter goed onder controle te houden, maar daardoor te beperkt om een zelfde soort selectie aan Lyapunov-exponenten te hebben als het wormsysteem. Ik denk dat het interessant is om de Nosé-Hoover oscillatoren nog verder te onderzoeken, en om dat te doen kan op de resultaten die ik hier heb worden voortgebouwd. Ook zijn er nog andere systemen die interessant zijn om te onderzoeken, zoals een (drie)dubbele slinger.

Contents

1	Introduction	6
1.1	The behavior of <i>C. elegans</i>	6
1.2	Behavior as a physical science	7
2	Theory	9
2.1	General theory of dynamical systems	9
2.1.1	Phase space and attractors	10
2.1.2	Chaotic systems and strange attractors	11
2.1.3	The spectrum of Lyapunov exponents	13
2.1.4	Hamiltonian systems	16
2.1.5	Conservative systems	16
2.1.6	Systems with viscous damping	17
2.2	<i>C. elegans</i> locomotion as a dynamical system	18
2.3	Constraining the model space	19
2.3.1	Multi-pendulum systems	19
2.3.2	Coupled chaotic oscillators	20
2.3.3	Nosé-Hoover oscillator	23
2.3.4	Periodically driven oscillators	24
3	Methods	26
3.1	Numerical evaluation of dynamical systems	26
3.2	Estimation of the Lyapunov exponents	27
3.2.1	Linear approximation and iteration of the flow	27
3.2.2	Volume scaling and the QR decomposition	29
3.2.3	Iteratively calculating the QR decomposition of F	31
3.2.4	Implementation of the algorithm	33
4	Results	35
4.1	Detailed calculation of the Lyapunov exponents	35
4.2	Lyapunov exponents of selected systems	38
4.3	Coupled Nosé-Hoover oscillators	41
5	Discussion	43
5.1	Accuracy of the calculations	43

5.2	Coupling the Nosé-Hoover oscillators	45
5.2.1	Symmetry of the coupled spectrum	46
5.3	The (damped) driven pendulum	49
5.4	Similarity to the <i>C. elegans</i> Lyapunov spectrum	50
6	Conclusion	52
7	Bibliography	54
A	Partial code for the Lyapunov exponents algorithm	56
B	Convergence plots	58

Introduction

1.1 The behavior of *C. elegans*

One of the most extensively studied organisms in biology is the worm *Caenorhabditis elegans* (or *C. elegans*), particularly in the field of neural biology, as it is one of the simplest organisms with a nervous system, and it is very suited to examination in experimental settings. As a result, its nervous system has been entirely mapped [2], and simulated [3].

A different story emerges when we consider the observable behavior of the worm. We see it perform a limited set of behaviors, that have been qualitatively categorized into several discrete behavioral states. However, what remains not well understood is how the structure of the brain of *C. elegans* gives rise to these behaviors. In spite of all efforts of examining the organism at the lowest level, its apparent liveliness remains an emergent phenomenon, unable to be reduced to the worm's constituent parts. And yet, from a qualitative point of view, there are clearly several 'modes' of behavior (i.e. forward and backward crawling, turning).

In the work of Greg Stephens et al. [4] an attempt has been made to understand the behavior in a different way. By quantitatively analyzing the two-dimensional locomotion of the worm, it has been found that its posture can be described in a very low dimensional space, which indicates that the behavior might be understood by investigating the dynamics in this *eigenworm* space [4]. While these dynamics are essentially generated by the neural structure of *C. elegans*, the main hypothesis of this analysis is that the emergent behavior can be described as a deterministic system consisting of fewer parts than neurons in the brain itself.

More generally, it is hypothesized that such complex systems of many interacting parts, which are perhaps not themselves well-understood, can be reasonably approximated as relatively simple chaotic dynamical systems. The ultimate goal would be to formulate a chaotic system of fewer parts that models the behavior of the complex system well. The

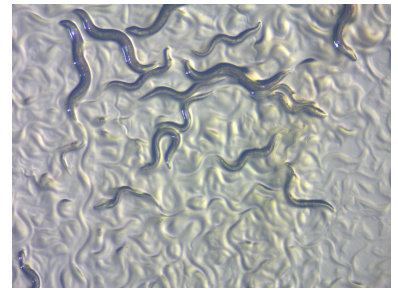


Figure 1.1: A number of crawling *C. elegans* worms imaged by a microscope. The individual worms are about 1 mm in length. Seen from above, we can see that their body shape is highly variable but seems semi-sinusoidal in most cases. This has been corroborated by the 'eigenworms'-analysis in [4]. Image from ZEISS Microscopy via Wikimedia Commons ([https://commons.wikimedia.org/wiki/File:C._elegans,_model_organism_in_life_sciences_\(28703152561\).jpg](https://commons.wikimedia.org/wiki/File:C._elegans,_model_organism_in_life_sciences_(28703152561).jpg)).

model complex system in this case is the worm *C. elegans*: specifically its autonomous locomotion when left undisturbed.

This project will build upon quantitative analysis that has been performed on the movement of *C. elegans* [1]. Among the results that have been obtained from this analysis is the **Lyapunov spectrum**, which describes certain characteristics of the dynamics of a system. The aim of this project is to construct one or more model systems that, when simulated, generate dynamics that give similar results for the Lyapunov spectrum. Ideally, these systems would have a clear origin from physics or other fields of science, so that they have a greater interpretability. This would make it possible to describe the dynamics of *C. elegans* qualitatively through **analogy**, which is often useful in physics as it leads to greater understanding¹.

1.2 Behavior as a physical science

The field of research in which this project takes place is often hard to categorize. This is because it concerns biological subjects (e.g. the worm), but is methodically very much like physics. Even more, it could be argued even the connection to physics is also vague, as it is simply the application of mathematical methods to biological phenomena. However, analogies can be made to physics that establish the connection more clearly. This connection is then mostly found in the methods applied, and how they are applied: while any (mathematical) science follows a systematic way of working, the constructs applied here and the way they are applied are characteristic of the way physics is performed as well.

The study of animal behavior (or *ethology*) as a physical science is well outlined in [5]. As mentioned there, the physical way of studying behavior is based on ‘outside’ observations (e.g. filmed behavior), and thus dependent on advances in computing technology (especially computer vision). Then, from these observations it is deduced what the relevant information is, in other words *what to measure*.

This is already one point that is often lacking in the study of behavior. As an example, let us look at an analogy to thermodynamics. Right now we have a quite extensive theory of temperature, for example the temperature of an (idealized) gas. First of all, we know it consists of particles trapped in a volume with a certain amount of kinetic energy. Then, this gas can (through collisions) transmit some energy, changing its entropy, and it is the way in which this happens which determines its temperature².

However, this is not how we usually think of temperature: it determines simply whether something feels hot or cold. This intuitive notion

¹ As an example, take the **electronic–hydraulic analogy**: a comparison can be made between water flowing through pipes and electricity moving through a circuit. This is because the water is governed by equations that have the same shape as the equations governing the electric charge.

This leads to a intuitive way of understanding what is happening in an electric circuit: we talk about the electricity ‘flowing’ through it, even though we cannot observe it doing so, and it is hard to say it is actually doing so in a literal sense. Interestingly enough, because of this correspondence it is also possible to build analog computers that run on water, e.g. the 1950’s MONIAC.

² Temperature is defined as

$$T = \left[\frac{\partial S}{\partial U} \right]^{-1}.$$

A gas with a high temperature (T) will give up energy more easily, which is the same as saying that a small change in energy (U) will not lead to a large change in entropy (S), so it is ‘easy’ for the gas to give up this energy.

of the right macroscopic quantity to measure makes it already possible to measure it, while not knowing much about the microscopic mechanisms, as the first thermometers were invented long before any other part of thermodynamics. However, in the case of behavior the macroscopic quantities to measure are much less clear, and the way of working is generally the other way around: we have quite a bit of knowledge of the microscopic picture (neurons), but have no quantitative grasp of the macroscopic behavior resulting from it. That would be like having a microscopic description of a gas as moving particles, possibly with a notion of entropy, but without having any idea of what temperature is. Now imagine someone asks you to derive some ‘laws’ that describe what happens in this gas: where do you start?

So with the research on ‘eigenworms’, an idea of how the observable behavior of *C. elegans* should be measured has been formed. The next question is: what kind of laws govern this behavior? Ultimately, these should follow from the microscopic description of the brain as well, but they are only useful if their effects are visible in the observable behavior. This makes it a good idea to analyze the behavior from a purely macroscopic standpoint as well: determining empirical laws before trying to discover where they come from. Because there is no clear cut way how to find ‘good’ laws from a set of observations, the idea behind this project is to look at existing systems whose structure has some motivation behind it, in order to get some inspiration for the kind of laws that could make the behavior observed in *C. elegans* emerge.

Theory

2.1 General theory of dynamical systems

In layman's terms, a **dynamical system** is “something that moves”. More generally, it is a system with properties that change as time progresses. For example, an object that moves through space may be described as having a position and a velocity as its dynamical properties. These properties change over time: ‘movement’ is essentially a change of position, and the velocity may also change through acceleration. But, many other systems that “move” in a different way may be described as dynamical systems as well¹.

The combined properties of an dynamical system with n properties are often called the **state** and described by a state vector

$$\vec{x} = \begin{pmatrix} x_1 \\ x_2 \\ \dots \\ x_n \end{pmatrix},$$

where $x_i, i \in \{1, \dots, n\}$ are the properties of the system. The way in which these properties change over time is then given by the time derivative

$$\frac{d\vec{x}}{dt} = \begin{pmatrix} \dot{x}_1 \\ \dot{x}_2 \\ \dots \\ \dot{x}_n \end{pmatrix} \equiv \dot{\vec{x}}.$$

also called the **flow** of the system.

Based on how the time derivative is defined, dynamical systems will be of one of two types²:

1. Systems in which $\dot{\vec{x}}$ can be modeled as a function $\dot{\vec{x}}(\vec{x})$ of the current state of the system, also called **autonomous systems**.

¹ Examples would be the current at a certain position in a circuit changing as the voltage is adjusted, or the population of a species changing due to environmental circumstances.

² The important difference between these two categories is that autonomous systems are completely predictable from the current state only, and so there is no need to know anything about what has happened in the past. For non-autonomous systems, external conditions can make a difference, for example whether the system is in a certain state for the first or the second time. This makes objective analysis of the behavior more difficult.

2. Systems in which $\dot{\vec{x}}$ can only be modeled as a function $\dot{\vec{x}}(\vec{x}, t)$ of both the current state and the current time. These systems are **non-autonomous**.

We'll consider non-autonomous systems, as they are more general.

Let's say the function f models the time evolution of the system, so that $\dot{\vec{x}} = f(\vec{x}, t)$. Then there is another way to divide these kind of systems into two types:

1. Systems in which we can write f as a vector of functions, each having only of the properties (and time) as input, i.e.

$$f(\vec{x}, t) = \begin{pmatrix} f_1(x_1, t) \\ f_2(x_2, t) \\ \dots \end{pmatrix}$$

so that $f_i(x_i, t) = \dot{x}_i$. As the equations $\dot{x}_i = f_i$ form a system of uncoupled differential equations, these systems are called **uncoupled systems**.

2. Systems for which the functions f_i have the entire state as input, i.e.

$$f(\vec{x}, t) = \begin{pmatrix} f_1(\vec{x}, t) \\ f_2(\vec{x}, t) \\ \dots \end{pmatrix}.$$

Here the set of equations $\dot{x}_i = f_i(\vec{x}, t)$ consists of coupled differential equations and therefore these systems are **coupled systems**.

In this project we will work with non-autonomous, coupled dynamical systems of the form:

$$\dot{\vec{x}} = \begin{pmatrix} \dot{x}_1 \\ \dot{x}_2 \\ \dots \\ \dot{x}_n \end{pmatrix} = f(\vec{x}, t) = \begin{pmatrix} f_1(\vec{x}, t) \\ f_2(\vec{x}, t) \\ \dots \\ f_n(\vec{x}, t) \end{pmatrix} \quad (2.1)$$

2.1.1 Phase space and attractors

The behavior of dynamical systems can be characterized by analyzing their **phase spaces**. The state of a system with n properties lives in an n -dimensional vector space. If we take states of the system that follow each other in time, plot them as points in this space, and connect them, we find a **trajectory** for the system. This is a path that describes how the system's state might change as time passes.

If we collect all possible trajectories, they collectively make up the phase space of the system. Useful remarks about the qualitative behavior

of the system can be made from knowing what kind of trajectories occur in this space, where trajectories go after a large period of time, and whether they are confined to a certain region in the phase space.

One important example of such a region is an **attractor**. This is a region in phase space into which nearby trajectories tend to move as time goes on. To be precise, an attractor is a region in phase space with two important properties [6]:

1. States contained in the attractor stay within the attractor.
2. There is some region B that is larger than the attractor for which all contained states move into the attractor eventually. The largest possible region B is called the basin of attraction.

Simple examples of attractors include sinks, single states into which nearby trajectories converge and remain forever, and stable limit cycles, closed loops (i.e. where the trajectory leads back into the same state after a while) onto which all nearby trajectories spiral eventually. However, some systems contain attractors with a more complex shape. These are called strange attractors and occur within systems whose behavior is classified as chaotic.

2.1.2 Chaotic systems and strange attractors

Chaotic systems are systems whose behavior is very unpredictable, because trajectories that start out close to each other, only stay close for a very short time. In other words, initially nearby states diverge very quickly.

Let's say the system starts in a state \vec{x}_1 and evolves for a time t into \vec{x}'_1 . If instead we start the system in a state $\vec{x}_2 \equiv \vec{x}_1 + \vec{\delta x}$ (where $\|\vec{\delta x}\|$ is small) and it evolves into \vec{x}'_2 , for a chaotic system it is the case that

$$\|\vec{\delta x}'\| = |\vec{x}'_2 - \vec{x}'_1| \gg |\vec{x}_2 - \vec{x}_1| = \|\vec{\delta x}\|.$$

Usually this divergence is approximately exponential, so that we can write the distance between points after a long time as

$$\|\vec{\delta x}'\| = e^{\lambda t} \|\vec{\delta x}\| \tag{2.2}$$

where λ is the **Lyapunov exponent**, which indicates how strong the divergence is [6]:

$$\lambda \equiv \frac{1}{t} \ln \left(\frac{\|\vec{\delta x}'\|}{\|\vec{\delta x}\|} \right). \tag{2.3}$$

Technically this equation is valid only in the limit $t \rightarrow \infty$, in which case it gives an notion of the average exponential divergence of trajectories per

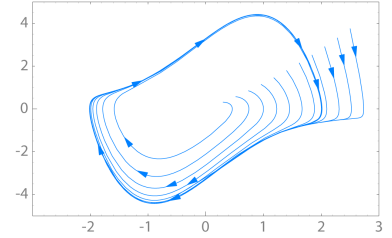


Figure 2.1: An example of a limit cycle: the attractor in the Van der Pol oscillator

$$f = \begin{bmatrix} \dot{x} \\ \dot{v} \end{bmatrix} = \begin{bmatrix} v \\ (1 - x^2)v - x \end{bmatrix}$$

visualized in (x, v) phase space. All trajectories eventually move onto the distinctive (non-harmonic) closed loop. From user XaosBits at Wikipedia.

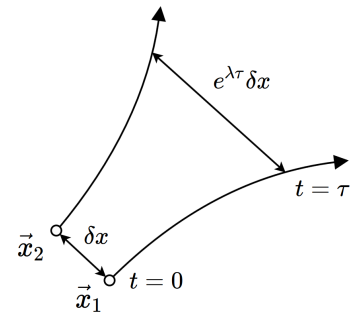


Figure 2.2: A visualization of exponential divergence in a system. The trajectories in phase space starting from \vec{x}_1 and \vec{x}_2 are initially separated by δx . The two trajectories then evolve so that this separation grows exponentially as a function of time, mediated by the Lyapunov exponent λ .

time unit. Systems that have a positive Lyapunov exponent for some set of parameters and initial conditions are classified as chaotic systems.

This exponential divergence of nearby states means the system's dependence on the initial conditions is very sensitive, and its behavior is unpredictable because similar scenarios cannot easily be compared, if at all. Exponential divergence also explains why these systems must have "strange" attractors: a sink leads to convergence ($|\vec{x}'_2 - \vec{x}'_1| = 0$) in the long term, and on a limit cycle the states will remain roughly equally separated ($|\vec{x}'_2 - \vec{x}'_1| \sim \mathcal{O}(\delta x)$) and thus there is no divergence.

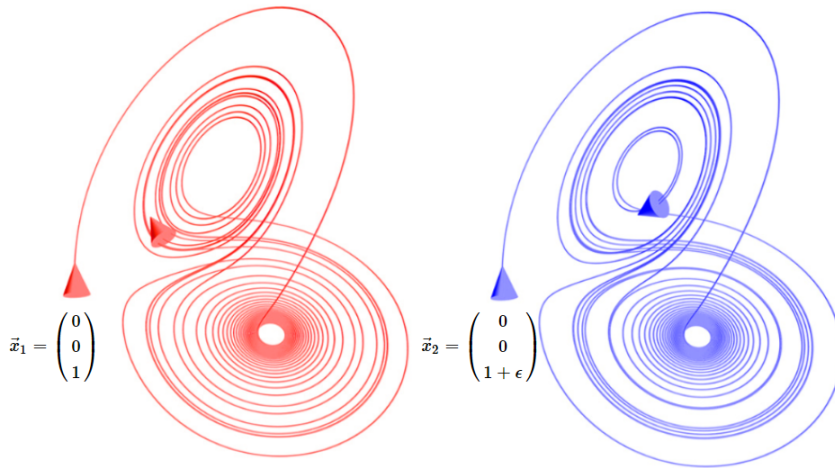


Figure 2.3: An example of exponential divergence: two trajectories in the Lorenz system

$$f = \begin{bmatrix} \dot{x} \\ \dot{y} \\ \dot{z} \end{bmatrix} = \begin{bmatrix} \sigma(y - x) \\ x(\rho - z) - y \\ xy - \beta z \end{bmatrix}$$

with parameters $(\sigma, \rho, \beta) = (10, 28, 8/3)$. The two trajectories start out very close, as

$$\delta x = \epsilon = 10^{-5},$$

but eventually end up quite dissimilar toward the end. From user XaosBits at Wikipedia.

Strange attractors are regions in phase space with an interesting geometric structure: they are fractals. This must be the case because of two seemingly contradictory properties. Let's say we have a region of initial states of a chaotic system that are within the basin of attraction of some attractor. Then it follows that:

1. This region shrinks into a region with zero volume as time passes.

First off, all attractors have zero volume³. For a region of states inside the basin of attraction that has a nonzero volume, these states must move ('flatten') onto the attractor and become a subset of the attractor set, which therefore has also zero volume.

2. This region grows in size exponentially with time.

The behavior of the system is chaotic, which means all the states inside this region will separate, and the distances between them will grow exponentially. Thus the size of the set containing the evolution of all these states will grow exponentially in size.

From this it follows that the attractor, being the object which contains the evolution of these states for all time, must have both zero volume, but

³ Attractors can only appear in dissipative systems [6], and thus $\nabla \cdot f < 0$ and volumes in phase space will always shrink over time.

also span an infinite distance. Fractals fit the bill, as these are objects with no volume, but infinite surface area. For this reason the fractal is a characteristic property for chaotic systems.

A way to understand how these fractals are formed, and thus how the time evolution of chaotic systems proceeds, is through the analogous transformations of stretching and folding. Stretching a region in phase space in one direction separates nearby states, leading to the exponential divergence. Then, contracting and folding this stretched region onto itself in the orthogonal subspace reduces the volume, and keeps the full set within a bounded region. Repeating this process infinitely many times reduces the ‘thickness’ of the region in at least one direction to zero, and thus the volume of the set of states goes to zero, while nearby states are still exponentially separated.

2.1.3 The spectrum of Lyapunov exponents

Since a chaotic system has exponential divergence of trajectories, and the Lyapunov exponent indicates how strong this divergence is, it is also a way to express how chaotic the system is. However, there are in fact n different Lyapunov exponents for a system with an n -dimensional phase space, because distance between states might be expanded in one direction (through stretching) but contracted in another (through folding). In fact, if there is an attractor, there must always be at least one negative exponent that makes sure the states stay on the attractor.

The set of all Lyapunov exponents for a system is called the **Lyapunov spectrum**. If we only look at how the distance between two points changes, we instead get the **maximum Lyapunov exponent**.

A way to formulate this mathematically is by looking at the deformation of a volume in phase-space. If we take a small m -dimensional region⁴ with volume V_0 of initial conditions and let it evolve according to the flow, we can characterize its volume scaling by m different exponents.

⁴ Where the dimension $m \leq n$, so that it fits in our phase space.

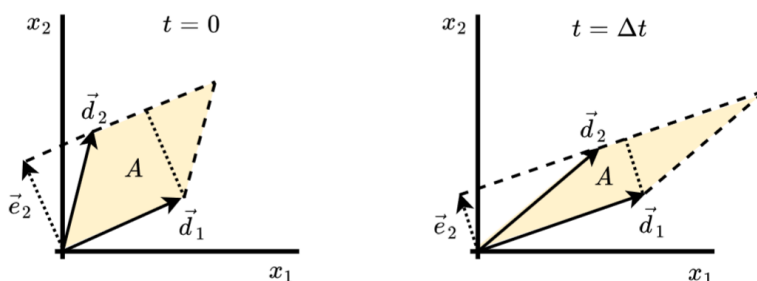


Figure 2.4: Two diagrams showing two distance vectors \vec{d}_1 and \vec{d}_2 , the parallelogram spanned by them and its area A , at both $t = 0$ and a later time Δt . The vector \vec{e}_2 orthogonal to \vec{d}_1 is also displayed. These two vectors span a rectangle that has the same area A .

To show this, we will look at a two-dimensional example. Consider an area spanned by two distance vectors \vec{d}_1 and \vec{d}_2 as in Figure 2.4. These two vectors form a parallelogram with area A . We can calculate this area if we construct a rectangle with equal area by calculating the vector \vec{e}_2 ,

which is equal to \vec{d}_2 minus the projection of \vec{d}_2 onto \vec{d}_1 . This makes it orthogonal to \vec{d}_1 , so that they form a rectangle whose area is given by multiplying their lengths. So if

$$\begin{aligned}\|\vec{d}_1\| &\equiv D_1 \\ \|\vec{d}_2\| &\equiv D_2 \\ \vec{e}_2 &= \vec{d}_2 - \frac{\vec{d}_2 \cdot \vec{d}_1}{\vec{d}_1 \cdot \vec{d}_1} \vec{d}_1 \\ \|\vec{e}_2\| &\equiv E_2(\vec{d}_2, \vec{d}_1),\end{aligned}$$

the area A is equal to

$$A = \|\vec{d}_1\| \|\vec{e}_2\| = D_1 \cdot E_2 \equiv A_0$$

Now, if we let the system evolve in time, the distance vectors \vec{d}_1 and \vec{d}_2 will grow according to the (largest) Lyapunov exponent λ_1 :

$$\begin{aligned}\|\vec{d}_1(\Delta t)\| &= D_1 e^{\lambda_1 \Delta t} \\ \|\vec{d}_2(\Delta t)\| &= D_2 e^{\lambda_1 \Delta t}.\end{aligned}$$

To calculate the new area A , we have to calculate a new vector \vec{e}_2 . Now, as in visible in Figure 2.4, \vec{e}_2 has not been scaled by the same factor $e^{\lambda_1 \Delta t}$. So if we want to describe how the area of this region in phase space changes, we also need to describe the growth of the orthogonal vector \vec{e}_2 . To do so we will introduce a second Lyapunov exponent λ_2 so that

$$\|\vec{e}_2(\Delta t)\| \equiv E_2 e^{\lambda_2 \Delta t}$$

and the new area A is equal to

$$\begin{aligned}A(\Delta t) &= \|\vec{d}_1(\Delta t)\| \|\vec{e}_2(\Delta t)\| \\ &= D_1 e^{\lambda_1 \Delta t} \cdot E_2 e^{\lambda_2 \Delta t} \\ &= A_0 e^{(\lambda_1 + \lambda_2) \Delta t},\end{aligned}$$

i.e., it is scaled by the sum of the two Lyapunov exponents.

This idea can be extended to higher-dimensional volumes, with each one adding an extra orthogonal vector whose growth we can consider and thus adding an extra exponent. This means the total volume change of an m -dimensional region with initial volume V_0 will be determined by the (sum of the) m largest Lyapunov exponents:

$$\lim_{t \rightarrow \infty} V_m(t) = V_0 \prod_{i=1}^m e^{\lambda_i t}$$

$$\begin{aligned} \lim_{t \rightarrow \infty} \ln(V_m(t)) &= \ln(V_0) + \sum_{i=1}^m \lambda_i t \\ \lambda_i^+ &\equiv \sum_{i=1}^m \lambda_i \\ &= \lim_{t \rightarrow \infty} \frac{1}{t} (\ln(V_m(t)) - \ln(V_0)) \\ &= \lim_{t \rightarrow \infty} \frac{1}{t} \ln \left(\frac{V_m(t)}{V_0} \right) \end{aligned} \tag{2.4}$$

Here we have defined λ_i^+ to be the sum of the m largest Lyapunov exponents.

The equation for the evolution of the distance between two nearby points is then given by the 1-dimensional case:

$$\lambda_1^+ = \lambda_1 = \frac{1}{t} \ln \left(\frac{V_1(t)}{V_0} \right) = \frac{1}{t} \ln \left(\frac{d(t)}{d_0} \right)$$

$$\text{and so, } d(t) = d_0 e^{\lambda_1 t}.$$

Equations for the individual exponents are obtained by looking at the difference between an m - and $(m-1)$ -dimensional region, both with initial volume V_0 :

$$\begin{aligned} \lambda_m &= \lambda_m^+ - \lambda_{m-1}^+ \\ &= \lim_{t \rightarrow \infty} \frac{1}{t} (\ln(V_m(t)) - \ln(V_0) - \ln(V_{m-1}(t)) + \ln(V_0)) \\ &= \lim_{t \rightarrow \infty} \frac{1}{t} \ln \left(\frac{V_m(t)}{V_{m-1}(t)} \right) \end{aligned} \tag{2.5}$$

One important result that can be obtained from the Lyapunov spectrum is the appearance of a zero-valued exponent. This exponent should appear in any dynamical system of the form as in Eq. 2.1. This is because when we analyse the divergence after a short time, two infinitesimally close states will never diverge in one particular direction: the direction in which the trajectories are moving at that instant. This is often called the direction ‘along the flow’. Therefore, the presence of a zero exponent is a necessary condition for the system to actually be continuous and deterministic. If there is no zero exponent, the system is either stochastic (there is no unique flow direction at every single instant) or discrete (so it is not well described by a set of dynamical equations, or possibly the phase space is incomplete).

Systems with more than one positive Lyapunov exponent are often called hyperchaotic. Because there is exponential divergence in more than one direction, the behavior will be even harder to predict, as the deterministic dynamics are visible only at increasingly short time scales [7].

2.1.4 Hamiltonian systems

Hamiltonian systems are a category of dynamical systems that are studied extensively in physics. This is partly because they can easily be used to describe a system that follows Newton's laws in a concise way, but they are also useful for modelling many other situations.

A Hamiltonian system has an even number of properties that come in pairs of q and p , respectively the generalized coordinate⁵ and the conjugate momentum⁶. Then there is a function $H(q, p, \dots)$, called the **Hamiltonian**, that relates these pairs of q and p as follows:

$$\begin{aligned} \frac{\partial q}{\partial t} &= \frac{\partial H}{\partial p} \text{ or } \dot{q} = H_p, \\ \frac{\partial p}{\partial t} &= -\frac{\partial H}{\partial q} \text{ or } \dot{p} = -H_q. \end{aligned} \tag{2.6}$$

⁵ An analogue of the position of objects in physical systems.

⁶ An analogue of the momentum, essentially the weighted velocity of objects.

In the language of dynamical systems this means a Hamiltonian system has the form

$$\dot{\vec{x}} = \begin{pmatrix} \dot{q}_1 \\ \dot{p}_1 \\ \dot{q}_2 \\ \dot{p}_2 \\ \dots \end{pmatrix} = f = \begin{pmatrix} H_{p_1} \\ -H_{q_1} \\ H_{p_2} \\ -H_{q_2} \\ \dots \end{pmatrix} \text{ where } H = H(\vec{x}).$$

2.1.5 Conservative systems

If the Hamiltonian H is not itself a function of time, the relations above can be used to show that

$$\frac{\partial H}{\partial t} = \frac{\partial H}{\partial q} \frac{\partial q}{\partial t} + \frac{\partial H}{\partial p} \frac{\partial p}{\partial t} = -\frac{\partial p}{\partial t} \frac{\partial q}{\partial t} + \frac{\partial q}{\partial t} \frac{\partial p}{\partial t} = 0.$$

This means the system described by H is **conservative**: the value of H is constant (conserved) across any trajectory⁷.

A slightly different but similar scenario is when the Hamiltonian varies over time, but does so periodically, i.e.

$$H(\vec{x}, t) = H(\vec{x}, t + T)$$

where T is its **conservation period**. Here, energy is not constant, but the average energy over a period T is conserved. We will call systems with a time-independent Hamiltonian **instantaneously conservative** and those with a periodic Hamiltonian **periodically conservative**.

In the context of dynamical systems a conservative system has the property that any region in phase space will retain a constant volume as time passes [6]. This implies that there can be no attractors in the

⁷ In physical systems, the value of H is usually the total energy of the system, which means a time-independent Hamiltonian indicates there is conservation of energy.

system, as there cannot be a basin of attraction that shrinks to the size of the attractor.

There is also an important symmetry in the Lyapunov exponents of a conservative system. Because any volume in phase space must stay constant, if this volume is stretched in any direction, it must be equally contracted in another direction as well. As the Lyapunov exponents show how the flow of time stretches or contracts any volume in phase space, this means for any positive Lyapunov exponent there must also be a negative exponent of equal size. Therefore, the Lyapunov exponents of a conservative system are symmetric around 0:

$$\lambda_i = -\lambda_{n+1-i} \quad (2.7)$$

with n the number of exponents, and $i = \{0, 1, \dots, n\}$ [8]. Additionally, because one exponent is always zero, and only $0 = -0$, there must be two zero exponents. Finally, the sum of all Lyapunov indicates the total expansion or contraction of the volume, and therefore has to be equal to zero:

$$\sum_i \lambda_i = 0. \quad (2.8)$$

These symmetries are also valid for periodically conservative systems, as the Lyapunov exponents are a time-averaged quantity [9].

2.1.6 Systems with viscous damping

Another important category of systems for this project is the category of conservative systems with the addition of a viscous damping force. Physically, a damping force (like friction) slows the system's movement, and is thus proportional to the momentum:

$$F_d \equiv -\gamma p$$

where γ is a coefficient that indicates the strength of damping. We can add this to our equations for Hamiltonian systems by adding F_d to the force term $F = dp/dt$:

$$p_t = -H_q - \gamma p$$

leading to the system

$$\dot{\vec{x}} = \begin{pmatrix} \dot{q}_1 \\ \dot{p}_1 \\ \dot{q}_2 \\ \dot{p}_2 \\ \dots \end{pmatrix} = f = \begin{pmatrix} H_{p_1} \\ -H_{q_1} - \gamma p_1 \\ H_{p_2} \\ -H_{q_2} - \gamma p_2 \\ \dots \end{pmatrix} \text{ where } H = H(\vec{x}). \quad (2.9)$$

The dynamical properties of this system differ from those of conservative systems in an intuitive way. Volumes in phase space are not constant, but shrink at a rate proportional to γ . From this it follows that the sum of the Lyapunov exponents is also proportional to γ . In fact, their sum is

$$\sum_i \lambda_i = -\frac{\gamma}{2}.$$

Finally, the same symmetry of Lyapunov exponents exists, except this time they are symmetric [9] around the value $-\frac{\gamma}{2}$:

$$\lambda_i + \frac{\gamma}{2} = -\left(\lambda_{n+1-i} + \frac{\gamma}{2}\right) \quad (2.10)$$

2.2 *C. elegans* locomotion as a dynamical system

Much analysis has been done on time series obtained from the movement data of *C. elegans* [1]. From this analysis a specific reconstruction of the phase space has emerged that provides a number of valuable insights.

First of all, using the method of false nearest neighbors, it has been established that the full *C. elegans* phase space can be very accurately reconstructed in 6 dimensions. In addition to that, singular value decomposition results in a particular basis in which the coordinate axes map neatly onto the three established discrete behaviors of forward movement, backward movement, and turning.

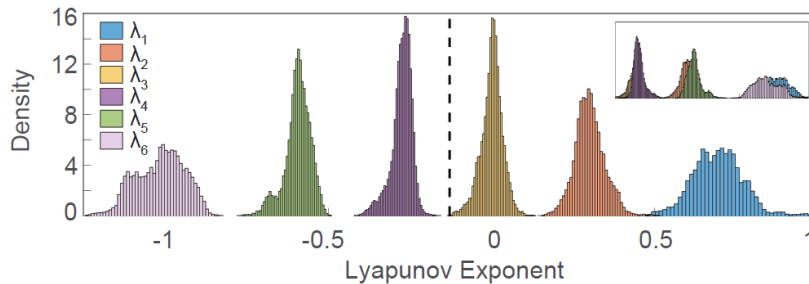


Figure 2.5: The estimated Lyapunov spectrum for *C. elegans* locomotion from [1]. It shows the cumulative distribution of the 6 LE's, calculated 1000 random phase space reconstructions. The spectrum can be separated in noisy distributions around 6 peaks, indicating there are 6 distinct exponents in these dynamics. They are approximately symmetric around the value indicated by the dashed line.

Finally, from this phase space reconstruction a Lyapunov spectrum has been calculated (Figure 2.5). This spectrum convincingly shows that there are 6 separate LEs, of which two are positive, one is zero, and three are negative. The zero exponent indicates that the trajectories indeed seem to follow a continuous, deterministic flow. Also, the Lyapunov spectrum is symmetric about a small negative value, which gives strong hints as to the structure of the eventual model.

As noted in Chapter 2.1.6, for conservative systems with viscous damping added it is exactly the case that their Lyapunov exponents are symmetric around a negative value (see Equation 2.10). This means that any

model for *C. elegans* behavior must be able to be expressed as a system that has viscous damping, but is otherwise conservative. We can check this numerically by looking at the Lyapunov spectrum, but we can also check this for models for which f is known by trying to formulate them using a Hamiltonian and the equations in Eq. 2.9.

2.3 Constraining the model space

When trying to find a model that fits the behavior of *C. elegans*, a good first step is to outline which kind of models could be up to the task. To do so we have to consider the global, qualitative behavior of different classes of models and then numerically investigate only those that show similar behavior as resulted from the analysis above.

The most general classification is the one in Equation 2.9, which is the class of conservative systems with viscous damping, limited to 6 dimensions. However, that leaves a large number of possible models for which no archetypal examples exist that can be enumerated systematically. Therefore the class of models should be narrowed down further before trying to find a model with suitable behavior. In the spirit of trying to find an understandable model, we will look at existing models that have a physical interpretation, and should be able to show qualitatively similar behavior.

2.3.1 Multi-pendulum systems

The first example of a physical model chaotic system that comes to mind is the **double pendulum**, consisting of a simple pendulum hanging off the end of another pendulum. When this pendulum is subjected to a periodic external force, its swinging motion can be chaotic. Alternatively, we can consider the **triple pendulum**, with another pendulum attached. This system shows hyperchaotic behavior [10], and is fully autonomous. An example of a chaotic trajectory of the triple pendulum is shown in Figure 2.6. Moreover, in a Hamiltonian formulation it is 6-dimensional (3 angles and 3 angular velocities) and conservative. Therefore, if we calculate its Lyapunov spectrum for a choice of parameters that shows chaotic behavior, it should be symmetric around 0. If we then add a uniform damping term, we should get a qualitatively similar spectrum to the *C. elegans* spectrum.

The upside of the triple pendulum is that it has a clear physical interpretation. However, its equations of motion are very complicated [11]. This makes it hard to integrate the system and to calculate the Lyapunov exponents. The same difficulties are also found in performing calculations for the double pendulum. One reason why is that the equations are hard

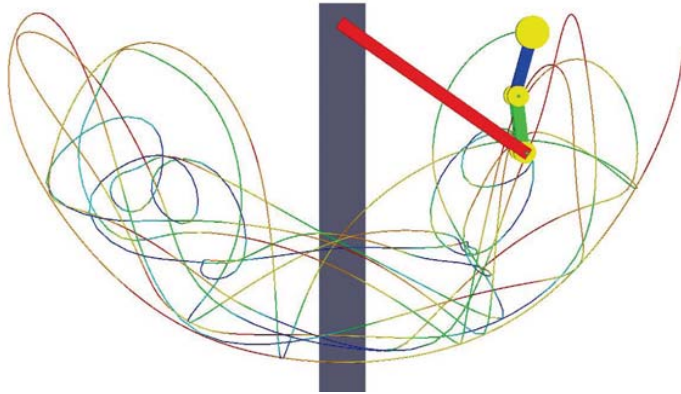


Figure 2.6: A chaotic trajectory for the triple pendulum from [11]. The Lyapunov exponents for this trajectory were found to be $\lambda_1 = 10.06$, $\lambda_2 = 1.85$, and $\lambda_3 = 0.00$ (rest given by symmetry). The parameters and equations of motion can be found in [11].

to integrate, because they are very sensitive to small errors in the integration. To generate a valid trajectory, an integrator must be used which incorporates energy conservation. Otherwise, the Lyapunov exponents for the system will be incorrect. Experimentally, it is observed that the zero exponents diverge. This added difficulty makes the multi-pendulum systems less suitable for this project, but as they can show a large range of behavior they provide an interesting pathway for future research.

2.3.2 Coupled chaotic oscillators

Another way to obtain the qualitative behavior sought after is by investigating **coupled chaotic oscillators**. If we have two 3-dimensional oscillators that show chaotic behavior (a positive Lyapunov exponent), embedding them in a 6-dimensional space will give a set of Lyapunov exponents that is simply the union of the single-oscillator sets of exponents. However, if we now couple the two oscillators, we expect one of the zero exponents will become negative, leading to a spectrum similar to the *C. elegans* spectrum, where two exponents are positive, one is zero, and three are negative. This transformation of the Lyapunov spectrum has been experimentally observed in coupled Rössler systems [12].

This situation can be engineered when coupling two harmonic oscillators by changing the equations in a specific way. If we have two harmonic oscillators described by four equations:

$$\begin{aligned} \dot{x}_{1,2} &= v_{1,2} \\ \dot{v}_{1,2} &= -kx_{1,2}, \end{aligned} \tag{2.11}$$

we can write down a Hamiltonian for this system:

$$H(x_1, v_1, x_2, v_2) = \frac{k}{2} \sum_{i=1}^2 x_i^2 + \frac{1}{2} \sum_{i=1}^2 v_i^2,$$

which shows that the system is conservative. Now in order to couple them in a way that preserves the symmetry of the Lyapunov spectrum,

there is only one way in which we can change the equations: by adding a uniform damping term to the velocities.

$$\begin{aligned}\dot{x}_{1,2} &= v_{1,2} \\ \dot{v}_{1,2} &= -kx_{1,2} - Cv_{1,2},\end{aligned}\tag{2.12}$$

where C is some constant. However, this does not couple the oscillators. An intuitive way to couple them from here would be to instead dampen the **phase velocity difference** $v_1 - v_2$, so that they attempt to synchronize their movements.

$$\begin{aligned}\dot{x}_{1,2} &= v_{1,2} \\ \dot{v}_{1,2} &= -kx_{1,2} - C(v_{1,2} - v_{2,1}),\end{aligned}\tag{2.13}$$

Now the question is: does coupling them in this way preserve the symmetry? For that to be the case, it must be possible to rewrite the equations in the form of Eq. 2.9, so in other words, the whole system *without* the damping terms must be Hamiltonian:

$$\begin{aligned}\dot{x}_{1,2} &= v_{1,2} \\ \dot{v}_{1,2} &= -kx_{1,2} + Cv_{2,1}\end{aligned}\tag{2.14}$$

$$H(x_1, v_1, x_2, v_2) = \dots$$

In order to write a Hamiltonian for the above system we will perform two coordinate transformations. First, we change to a basis of

$$\begin{aligned}x_{+,-} &= x_1 \pm x_2 \\ v_{+,-} &= v_1 \pm v_2,\end{aligned}$$

so that the equations become

$$\begin{aligned}\dot{x}_{+,-} &= \dot{x}_1 \pm \dot{x}_2 = v_{+,-} \\ \dot{v}_+ &= \dot{v}_1 + \dot{v}_2 = -k(x_1 + x_2) + C(v_2 + v_1) = -kx_+ + Cv_+ \\ \dot{v}_- &= \dot{v}_1 - \dot{v}_2 = -k(x_1 - x_2) + C(v_2 - v_1) = -kx_- - Cv_-\end{aligned}\tag{2.15}$$

One aspect of note is that in this basis the equations are symmetric. While the equation for v_- has a damping term (-C), the equation for v_+ has a *inverted* (+C) damping term. This already seems to implicate that energy is conserved between these two quantities.

If we compare these equations the ones in [13], we see that they are the same as the equation for a damped harmonic oscillator together with what is in their case an auxillary equation. This means we can use the same approach in writing a Hamiltonian for this system. If the second

coordinate transformation is performed as:

$$\begin{aligned} q_{1,2} &= x_{+,-} \\ p_2 &= v_+ \\ p_1 &= v_- - Cx_-, \end{aligned} \tag{2.16}$$

we can write down the Hamiltonian

$$H(q_1, p_1, q_2, p_2) = p_1 p_2 + k q_1 q_2 - C q_2 p_2$$

from which the equations of motion are derivable by choosing the pairs (q_i, p_i) as positions with conjugate momenta.⁸ The following equations are then obtained:

⁸ Note that the definitions of q and p are ‘swapped’, so that q_1 corresponds to x_+ but p_2 corresponds to its time derivative v_+ .

$$\begin{aligned} \dot{q}_1 &= H_{p_1} = p_2 \\ \dot{p}_1 &= -H_{q_1} = -k q_2 \\ \dot{q}_2 &= H_{p_2} = p_1 - C q_2 \\ \dot{p}_2 &= -H_{q_2} = -k q_1 + C p_2, \end{aligned} \tag{2.17}$$

for which substituting variables as in (2.16) shows that these are the same equations as in (2.15), and therefore they describe the same system as in (2.14). This shows the coupled system without damping is Hamiltonian, and its conserved quantity in $(x_{1,2}, v_{1,2})$ -space is

$$H = v_1^2 - v_2^2 + k(x_1^2 - x_2^2).$$

The only question that remains is, what happens when we add the damping? To do this properly, we should work backwards from the q, p coordinates and find the right equations for $\dot{v}_{1,2}$. We can make the following adjustment while preserving symmetry:

$$\begin{aligned} \dot{q}_1 &= H_{p_1} = p_2 \\ \dot{p}_1 &= -H_{q_1} - C p_1 = -k q_2 - C p_1 \\ \dot{q}_2 &= H_{p_2} = p_1 - C q_2 \\ \dot{p}_2 &= -H_{q_2} - C p_2 = -k q_1, \end{aligned} \tag{2.18}$$

for which a substitution of variables shows that the corresponding equations for x and v are

$$\begin{aligned} \dot{x}_{1,2} &= v_{1,2} \\ \dot{v}_{1,2} &= -k x_{1,2} + C v_{2,1} - \frac{C^2}{2} (x_{1,2} - x_{2,1}). \end{aligned} \tag{2.19}$$

This leads us to conclude the right way to couple two oscillators while

preserving symmetry is as follows:

$$\begin{aligned} \dot{x}_{1,2} &= v_{1,2} \\ \dot{v}_{1,2} &= -kx_{1,2} - C(v_{1,2} - v_{2,1}) - \frac{C^2}{2}(x_{1,2} - x_{2,1}). \end{aligned} \tag{2.20}$$

It is argued that this same principle might also hold when coupling other (chaotic) oscillators, leading to a conservative system with an effective added damping. In that case, coupling two 3-D conservative chaotic oscillators should lead to a spectrum qualitatively similar to the *C. elegans* spectrum. In the following sections, two conservative oscillating systems are considered as candidates for investigation into their behavior after coupling.

2.3.3 Nosé-Hoover oscillator

The Nosé-Hoover oscillator is a model for the interaction between a Hamiltonian system embedded in a heat bath at constant temperature, often used for simulations of molecular dynamics. It is conservative (energy is only exchanged between heat bath and the molecular system) so that the Lyapunov spectrum is symmetric [14]. It can be described as a three-dimensional dynamical system:

$$f = \begin{pmatrix} \dot{x} \\ \dot{v} \\ \dot{s} \end{pmatrix} = \begin{pmatrix} v \\ -x - vs \\ a(v^2 - 1) \end{pmatrix} \tag{2.21}$$

where x represents position, v velocity or momentum, and s is the effective friction imposed by the heat bath.

These equations are obtained from a nondimensionalization of a $(2n + 2)$ -dimensional Hamiltonian system of oscillating particles (2 variables each) with an extra heat bath ‘particle’ (with its own position and momentum) which is kept at a constant temperature, with which the other particles can exchange energy. It is used in chemical simulations to keep the temperature of a large ensemble of particles constant, so this extra heat bath component is also called a thermostat.

This system exhibits chaotic behavior, and is one of the simplest examples of a 3-dimensional system that does so [15]. It also has a nice physical origin related to statistical mechanics, which gives it a connection to the subtly varying behavior of a system kept at a temperature that is constant on average but fluctuates on short time scales.

The behavior of coupled instances of this system has been studied [16], but not in the context of dynamical systems and related properties, so this makes it an interesting direction for numerical investigation.

To couple these systems in a way that is similar to both the previous

section on coupled harmonic oscillators (hopefully preserving symmetry) and to the coupling in [12], the following system specification is used:

$$\dot{\vec{x}} = \begin{pmatrix} \dot{x}_1 \\ \dot{v}_1 \\ \dot{s}_1 \\ \dot{x}_2 \\ \dot{v}_2 \\ \dot{s}_2 \end{pmatrix}, \quad (2.22)$$

$$\begin{aligned} \dot{x}_{1,2} &= v_{1,2} \\ \dot{v}_{1,2} &= -k_{1,2}x_{1,2} - v_{1,2}s_{1,2} - C(v_{1,2} - v_{2,1}) - \frac{C^2}{2}(x_{1,2} - x_{2,1}) \\ \dot{s}_{1,2} &= a(v_{1,2}^2 - 1). \end{aligned} \quad (2.23)$$

Here the coupling between two instances is performed just as with the harmonic oscillators, and a new ‘spring constant’ parameter $k_{1,2}$ is added. In this way, we can make the oscillation frequencies of the oscillators slightly dissimilar, just as in [12].

2.3.4 Periodically driven oscillators

Another category of oscillators that can show chaotic behavior are driven oscillators. The simplest example is a pendulum that is affected (driven) by a periodic force,

$$\ddot{\phi} + \sin(\phi) = \sin(t).$$

This oscillator shows chaotic behavior for a large number of initial conditions (see Figure 2.7) [17]. We can write it as a Hamiltonian system by using the Hamiltonian

$$H(p, q, t) = \frac{p^2}{2} - \cos(q) - q \sin(t),$$

where $q \equiv \phi$ and $p \equiv \dot{\phi} \equiv \omega$. This Hamiltonian is periodic with period $T = 2\pi$, so this is a periodically conservative system and the desired symmetry of the Lyapunov spectrum applies to this system.

If we express this oscillator as a dynamical system, it is non-autonomous because of the explicit dependence on t . We can make it autonomous by introducing a third variable:

$$f = \begin{pmatrix} \dot{\phi} \\ \dot{\omega} \\ \dot{\tau} \end{pmatrix} = \begin{pmatrix} \omega \\ \sin(\tau) - \sin(\phi) \\ 1 \end{pmatrix} \quad (2.24)$$

Because the driving signal here is simple, we can also write this system

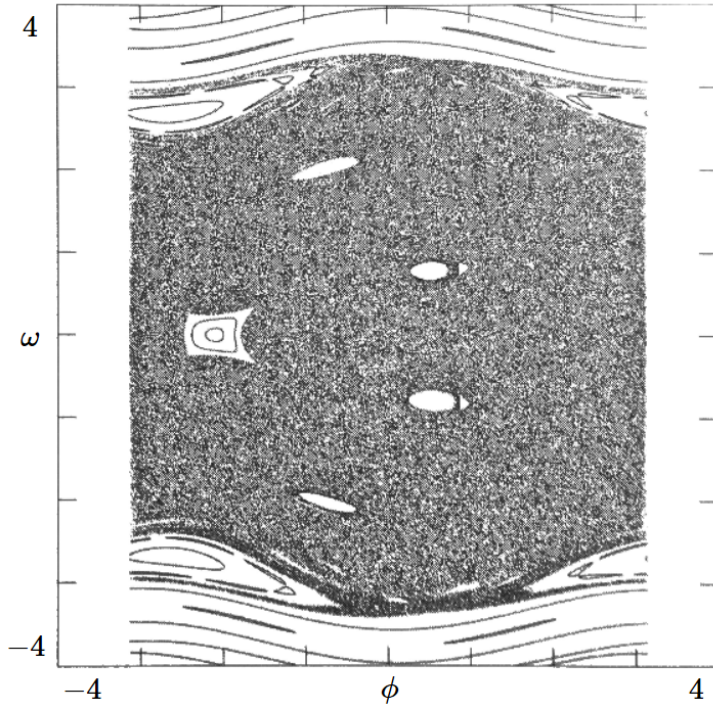


Figure 2.7: The *Poincaré section* for the driven pendulum in Eq. 2.24, from [17]. This shows a ‘slice’ of the phase space, namely the values of ϕ and ω whenever $\tau = \frac{\pi}{2} \pmod{2\pi}$ during a trajectory. The dots covering almost the entire space show that a trajectory going through one of the dots might re-enter the slice at almost any other point, indicating the non-periodic shape of the trajectories. There are only a few empty regions of initial conditions, indicating periodic trajectories occur there instead.

as a unidirectionally coupled system of two oscillators. If a system with equations

$$f = \begin{pmatrix} \dot{\phi}_2 \\ \dot{\omega}_2 \end{pmatrix} = \begin{pmatrix} \omega_2 \\ -\phi_2 \end{pmatrix} \quad (2.25)$$

is started with the initial conditions $(\phi_2, \omega_2) = (0, 1)$, it will generate the output signal (i.e. a solution of the system will be) $\phi(t) = \sin(t)$ ⁹. Therefore we can rewrite Eq. (2.24) as

$$f = \begin{pmatrix} \dot{\phi}_1 \\ \dot{\omega}_1 \\ \dot{\phi}_2 \\ \dot{\omega}_2 \end{pmatrix} = \begin{pmatrix} \omega_1 \\ \phi_2 - \sin(\phi_1) \\ \omega_2 \\ -\phi_2 \end{pmatrix}, \quad (2.26)$$

which is a system of a harmonic oscillator driving a pendulum. If this system is given the mentioned initial conditions for (ϕ_2, ω_2) , its behavior should be equivalent to the system in Eq. (2.24).

Other examples which are based on different conservative oscillators are mentioned in [17]. As many of these systems exhibit chaotic behavior, a coupling of two systems of this kind should result in a system with the desired Lyapunov spectrum, given the right parameters. It also provides a large class of systems to enumerate.

⁹This is just a harmonic oscillator so its solution is assumed common knowledge.

Methods

3.1 Numerical evaluation of dynamical systems

If we have a dynamical system defined by a flow function f , we cannot straightforwardly investigate its properties by looking at the equations. To plot the phase space, or to calculate Lyapunov exponents, we need to know what trajectories the system follows. For any dynamical system, we can obtain a set of these trajectories by **numerical integration**. We pick one or a set of **initial conditions** \vec{x}_0 , and iteratively use the value of \vec{x} given by $f(\vec{x})$ to calculate the ‘next’ point in phase space, after a small discrete time step.

There are several techniques to calculate the value $\vec{x}[t + \Delta t]$ (after a time step Δt), from the equation $\dot{\vec{x}} = f(\vec{x})$ and the current value of $\vec{x}[t]$. The simplest is called the (forward) **Euler method**, and simply uses the value of f as a constant derivative (i.e. a linear slope):

$$\vec{x}[t + \Delta t] = \vec{x}[t] + \Delta t \cdot f(\vec{x}[t]).$$

This is a linear method, which means that the error (i.e. the distance from the actual function $x(t)$) is proportional to the **step size** Δt . This means a very small step size is necessary for accurate calculation of a trajectory. A simple improvement of the accuracy can be made by using the (explicit) **midpoint method**. Here the derivative $\dot{\vec{x}}$ is evaluated at $t + \Delta t$ by using a regular Euler step, and then the derivative used in the actual evaluation is the average of $\dot{\vec{x}}$ at t and at $t + \Delta t$.

$$\begin{aligned}\dot{\vec{x}}_1 &\equiv f(\vec{x}[t]), \\ \dot{\vec{x}}_2 &\equiv f(\vec{x}[t] + \Delta t \cdot \dot{\vec{x}}_1), \\ \vec{x}[t + \Delta t] &= \vec{x}[t] + \frac{\dot{\vec{x}}_1 + \dot{\vec{x}}_2}{2} \Delta t.\end{aligned}$$

This essentially approximates the linear slope halfway between t and at $t + \Delta t$. This method is also known as the second-order **Runge-Kutta**

method, as part of a family of higher-order methods. Even more accurate, and often used, is the fourth-order method **RK4**, which works by calculating 4 midway derivatives:

$$\begin{aligned}\dot{\vec{x}}_1 &\equiv f(\vec{x}[t]), \\ \dot{\vec{x}}_2 &\equiv f(\vec{x}[t] + 0.5\Delta t \cdot \dot{\vec{x}}_1), \\ \dot{\vec{x}}_3 &\equiv f(\vec{x}[t] + 0.5\Delta t \cdot \dot{\vec{x}}_2), \\ \dot{\vec{x}}_4 &\equiv f(\vec{x}[t] + \Delta t \cdot \dot{\vec{x}}_3), \\ \vec{x}[t + \Delta t] &= \vec{x}[t] + \frac{\dot{\vec{x}}_1 + 2\dot{\vec{x}}_2 + 2\dot{\vec{x}}_3 + \dot{\vec{x}}_4}{6}\Delta t.\end{aligned}$$

In any case, when performing numerical integration very small numbers are used, for example in the time step Δt . To avoid rounding errors, whenever these small numbers are added to a large number¹ a compensation algorithm such as **Kahan summation**² should be used.

¹ For example in calculating $t + \Delta t$, because t will grow large while Δt will remain a small number.

3.2 Estimation of the Lyapunov exponents

3.2.1 Linear approximation and iteration of the flow

As noted in Chapter 2.1.3, the full Lyapunov spectrum consists of n exponents for a n -dimensional system. These emerge when considering how the volume of an n -dimensional region changes when it is deformed under the flow f .

In this section we will derive a more explicit formula for the Lyapunov exponents which can be used to program an algorithm to calculate them. The Lyapunov exponents come into play when looking at how the distance between nearby points converged or diverges as time elapses.

We will consider two nearby points \vec{p}_1 and \vec{p}_2 and their distance vector $\vec{d} = \vec{p}_2 - \vec{p}_1$ which has a small initial size $\|\vec{d}\| = d_0 \ll 1$. Its time evolution looks like

$$\dot{\vec{d}} = \dot{\vec{p}}_2 - \dot{\vec{p}}_1 = f(\vec{p}_2) - f(\vec{p}_1).$$

Now, we make an approximation: we're investigating the dynamics of a small distance d_0 , so it suffices to look at the local linear approximation of f . We'll call this function f_l .

We can find an expression for f_l by Taylor-expanding it around \vec{p}_1 :

$$[f_l]_i(\vec{p}) = f_i(\vec{p}_1) + \frac{\partial f_i}{\partial x_j}(\vec{p}_1) ([\vec{p}]_i - [\vec{p}_1]_i). \quad (3.1)$$

Here $[v]_i$ signifies the i -th component of the vector (or vector function) v , and there is an implicit sum over all phase-space coordinates x_j .

² Kahan summation works by comparing the value *after* summing to the largest value before. As the change may be negligible because of limited precision, a compensation value will be tracked in order to 'bundle' successive additions into a larger number which may be added properly. In this way the successive rounding errors will not add up over time.

Using this to express the time evolution of \vec{d} gives:

$$\begin{aligned}
 \left[\dot{\vec{d}}\right]_i &\approx [f_i]_i(\vec{p}_2) - [f_i]_i(\vec{p}_1) \\
 &= f_i(\vec{p}_1) + \frac{\partial f_i}{\partial x_j}(\vec{p}_1) ([\vec{p}_2]_i - [\vec{p}_1]_i) - f_i(\vec{p}_1) - \frac{\partial f_i}{\partial x_j}(\vec{p}_1) ([\vec{p}_1]_i - [\vec{p}_1]_i) \\
 &= \frac{\partial f_i}{\partial x_j}(\vec{p}_1) ([\vec{p}_2]_i - [\vec{p}_1]_i) \\
 &= \frac{\partial f_i}{\partial x_j}(\vec{p}_1) [\vec{d}]_i.
 \end{aligned}$$

From this we get the definition of the **Jacobian**, which is a matrix \mathbf{J} with entries

$$\mathbf{J}_{ij} = \frac{\partial f_i}{\partial x_j}(\vec{p}_1),$$

so that

$$\dot{\vec{d}} \approx \mathbf{J}\vec{d}.$$

This matrix represents the linearized flow of the system near point \vec{p}_1 . In order to find the Lyapunov exponents, we should study not the flow, but the effect the flow has over a long time (i.e. in the near-infinite time limit). To do so, we can construct the **flow map**

$$\mathbf{M} = \mathbf{I} + \Delta t \mathbf{J},$$

which is a matrix that when applied to a distance vector \vec{d} maps it a time Δt forward into time:

$$\mathbf{M}\vec{d}(t) = \vec{d}(t) + \Delta t \mathbf{J}\vec{d}(t) \approx \vec{d}(t) + \dot{\vec{d}}(t) \cdot \Delta t \approx \vec{d}(t + \Delta t)$$

Here the time step Δt needs to be small, because we have chosen to only use a linear timestep, so again this is an approximation. Also, for each point \vec{p} in the trajectory and thus for each time step the Jacobian and the flow map need to be recalculated, because the local flow may differ from point to point.

Using the maps $\mathbf{M}(t)$ we can iterate the distance vector from the beginning of the trajectory to some time $t = n\Delta t$:

$$\begin{aligned}
 \vec{d}(t) &= \vec{d}(n\Delta t) \\
 &= \mathbf{M}(\vec{p}([n-1]\Delta t))\vec{d}([n-1]\Delta t) \\
 &= \mathbf{M}(\vec{p}([n-2]\Delta t))\mathbf{M}(\vec{p}([n-1]\Delta t))\vec{d}([n-2]\Delta t) \\
 &= \prod_{i=n-1}^0 \mathbf{M}(\vec{p}(i\Delta t))\vec{d}(0).
 \end{aligned}$$

To simplify the notation the Jacobian will now be called $\mathbf{J}_n = \mathbf{J}(\vec{p}(n\Delta t))$ and the flow map $\mathbf{M}_n = \mathbf{M}(\vec{p}(n\Delta t))$ to signify they are based around the point $\vec{p}(n\Delta t)$ that occurs in the trajectory after taking n time steps. Then

the iteration becomes:

$$\vec{x}(t) = \prod_{i=n-1}^0 M_i \vec{x}(0),$$

where $t = n \cdot \delta t$.

Now, if we have a trajectory of N time steps, the matrix product $M_{N-1}M_{N-2}\dots M_0$ will tell us about the full evolution of a distance vector \vec{d} along the trajectory. We will therefore define

$$\mathbf{F} \equiv \prod_{i=N-1}^0 M_i$$

as the **integrated flow matrix**. In our numerical investigation, keeping track of the transformed volume along the entire trajectory is the nearest we can get to the infinite-time limit for the calculation of the Lyapunov exponents as in Eqs. 2.4 and 2.5. We can therefore investigate the volume-expanding or contracting properties of this matrix to generate an estimate for the Lyapunov exponents. The next section will describe an algorithm that computes this matrix iteratively and uses it to estimate the exponents.

3.2.2 Volume scaling and the QR decomposition

To find the Lyapunov exponents, we are interested in what the long-time behavior of volumes in phase space is. For this we need to calculate what the volume-scaling effect is of the matrix \mathbf{F} .

We start with an n -dimensional object (where n is the dimension of our phase space): an ‘identity volume’, which is an n -parallelepiped spanned by the column vectors of the identity matrix \mathbf{I}_n . This object has two nice properties: its initial volume $V_0 = 1$, as the determinant of the identity matrix is 1. Additionally, the final volume is given by $\mathbf{F}\mathbf{I}_n = \mathbf{F}$, i.e. the volume of the object spanned by the columns of \mathbf{F} . Therefore the volume $\lim_{t \rightarrow \infty} V_n(t)$ will be approximated by this volume.

To view the volume-scaling behavior of \mathbf{F} , we can perform a QR-decomposition of the matrix. This decomposition splits \mathbf{F} into the product of a \mathbf{Q} , which is orthogonal³, and a \mathbf{R} , which is upper triangular⁴. This is already a very useful decomposition for us, as the matrix \mathbf{Q} will be volume-preserving, and therefore does not affect the change in volume of our object. Secondly, the matrix \mathbf{R} is upper triangular, which means its effect on the volume can easily be calculated by taking the product of the values on its diagonal. Therefore the change in volume can be calculated

³ An orthogonal matrix \mathbf{Q} has column vectors that are each orthogonal to one another, and have length 1. This means that the matrix is volume-preserving (its determinant is 1), and its transpose \mathbf{Q}^T is also its inverse, so that $\mathbf{Q}^T\mathbf{Q} = \mathbf{Q}\mathbf{Q}^T = \mathbf{I}$.

⁴ An upper triangular matrix \mathbf{U} has only zero entries below the diagonal, i.e., only the entries on and above the diagonal are nonzero. The general form is:

$$\mathbf{U} = \begin{bmatrix} u_{1,1} & u_{1,2} & \dots & u_{1,n} \\ 0 & u_{2,2} & \dots & u_{2,n} \\ \vdots & \ddots & \ddots & \vdots \\ 0 & \dots & 0 & u_{n,n} \end{bmatrix}.$$

This means it has some useful properties, one being that its determinant is given by the product of its diagonal values.

as

$$\begin{aligned}
 \lim_{t \rightarrow \infty} V_n(t) &\approx \det(\mathbf{F}) \cdot V_0 \\
 &= \det(\mathbf{F}) \cdot 1 \\
 &= \det(\mathbf{Q}) \det(\mathbf{R}) \\
 &= 1 \cdot \det(\mathbf{R}) \\
 &= \prod_{i=0}^n R_{ii}
 \end{aligned}$$

We can visualize these transformations by performing a further decomposition. Note that the matrix \mathbf{R} consists of a scaling part (the diagonal, giving rise to equations such as $x_{t+1} = c \cdot x_t$) and a shearing part (the values above the diagonal, giving rise to equations such as $x_{t+1} = x_t + c \cdot y_t$). We can separate these by constructing a diagonal matrix \mathbf{D} containing the same diagonal as \mathbf{R} ,

$$D_{ij} = \begin{cases} R_{ij} & \text{if } i = j, \\ 0 & \text{if } i \neq j, \end{cases}$$

and then using its inverse \mathbf{D}^{-1} to calculate $\mathbf{S} = \mathbf{R}\mathbf{D}^{-1}$, so that:

$$\mathbf{F} = \mathbf{Q}\mathbf{R} = \mathbf{Q}\mathbf{R}\mathbf{D}^{-1}\mathbf{D} = \mathbf{Q}\mathbf{S}\mathbf{D}.$$

This separates \mathbf{F} into three transformations, first scaling by \mathbf{D} , then shearing by \mathbf{S} , then a rotation or mirroring by \mathbf{Q} . Also, note the diagonal of \mathbf{S} has only ones because of its definition, so that $\det(\mathbf{F}) = \det(\mathbf{D})$ and the volume scaling part is clearly contained in \mathbf{D} (or the diagonal of \mathbf{R}).

For a $(n - 1)$ -dimensional volume, we can consider the object spanned by the first $n - 1$ columns of \mathbf{I}_n , which we will call $\tilde{\mathbf{I}}_{n-1}$. The resulting volume is then given by $\mathbf{R}\tilde{\mathbf{I}}_{n-1}$ which is equal to the first $n - 1$ columns of \mathbf{R} concatenated, which we will call $\tilde{\mathbf{R}}_{n-1}$. This matrix represents a $(n - 1)$ -dimensional object in n -dimensions, which understandably has zero volume, as it is flat in the n -th dimension⁵. However, to consider the volume in the first $(n - 1)$ -dimensions, we can truncate the last row from $\tilde{\mathbf{R}}_{n-1}$ and $\tilde{\mathbf{I}}_{n-1}$ to obtain \mathbf{R}_{n-1} and \mathbf{I}_{n-1} . This does not change the shape of the object, as in both cases no column has a nonzero component in the last dimension (i.e. the last row is all zeroes). Then, we again have

⁵ Note that the determinant also doesn't exist, as it is not a square matrix.

$V_0 = \det(I_{n-1}) = 1$ and

$$\begin{aligned} \lim_{t \rightarrow \infty} V_{n-1}(t) &\approx \det(\mathbf{R}_{n-1}) \\ &= \prod_{i=0}^{n-1} [R_{n-1}]_{ii} \\ &= \prod_{i=0}^{n-1} R_{ii}, \end{aligned}$$

so the final volume is given by the product of the first $n - 1$ values on the diagonal of R .

Repeating this process for $n - 2$ dimensions, $n - 3$ dimensions, until 1 dimension, gives the result that for any $m \leq n$:

$$\lim_{t \rightarrow \infty} V_m(t) \approx \prod_{i=0}^m R_{ii}.$$

Then an equation for the Lyapunov exponents follows by substituting into Eq. (2.5):

$$\begin{aligned} \lambda_m &= \lim_{t \rightarrow \infty} \frac{1}{t} \ln \left(\frac{V_m(t)}{V_{m-1}(t)} \right) \\ &\approx \frac{1}{N\Delta t} \ln \left(\frac{\prod_{i=0}^m R_{ii}}{\prod_{i=0}^{m-1} R_{ii}} \right) \\ &= \frac{1}{N\Delta t} \ln(R_{mm}). \end{aligned} \tag{3.2}$$

3.2.3 Iteratively calculating the QR decomposition of F

To calculate the R -part of F , we of course first have to calculate F itself. However, this leads to numerical errors, as the indices of F can get very big and so we lose precision when taking the average in the end. For example, if each time step scales the volume by a factor 1.22 (corresponding to a (discrete) Lyapunov exponent of about 0.2), after 50000 time steps the cumulative scaling factor will be $1.22^{50000} \approx 9.8 \cdot 10^{4317}$. Involving numbers this large will lead to a loss of precision. Instead, we would like to calculate (the diagonal values of) R in an iterative way, so that we can keep track of a moving average which will always be similar in size to the final value of the exponent.

We can write F as the product

$$F = M_{N-1}M_{N-2}\dots M_1M_0$$

so an intuitive way would be to decompose each M_i into $M_i = Q_iR_i$.

However, this leads to a sequence of

$$F = Q_{N-1}R_{N-1}Q_{N-2}R_{N-2}\dots Q_1R_1Q_0R_0 = QR$$

which does not help in calculating the final value of R , as $Q_iR_i \neq R_iQ_i$

and so we still need to calculate the full product. We would like to have a sequence of Qs followed by Rs, so that

$$F = Q_{N-1}Q_{N-2}\dots Q_1Q_0R_{N-1}R_{N-2}\dots R_1R_0 = QR$$

which implies

$$\begin{aligned} Q &= Q_{N-1}Q_{N-2}\dots Q_1Q_0 \\ R &= R_{N-1}R_{N-2}\dots R_1R_0, \end{aligned}$$

as the product of orthogonal matrices is itself a orthogonal matrix, and the product of upper triangular matrices is also a upper triangular matrix.

A different way to calculate F iteratively is as follows. Starting with M_0 , we can just decompose this as

$$M_0 \equiv Q_0R_0.$$

Then, we can rewrite the product M_1M_0 as follows:

$$\begin{aligned} M_1M_0 &= IM_1M_0 = Q_0Q_0^T M_1M_0 \\ &= Q_0Q_0^T M_1Q_0R_0 \\ &\equiv Q_0Q_1R_1R_0. \end{aligned}$$

Here we have used the fact that Q_0 is orthogonal and so $Q_0Q_0^T = I$, and also decomposed $Q_0^T M_1Q_0$ into Q_1R_1 . We can repeat this process for the product $M_2M_1M_0$:

$$\begin{aligned} M_2M_1M_0 &= Q_0Q_1(Q_0Q_1)^T M_2M_1M_0 \\ &= Q_0Q_1(Q_0Q_1)^T M_2Q_0Q_1R_1R_0 \\ &\equiv Q_0Q_1Q_2R_2R_1R_0. \end{aligned}$$

From this we get the iterative sequence:

$$\begin{aligned} Q_0R_0 &= M_0 \\ \hat{Q}_n &\equiv \prod_{i=0}^n Q_i \\ Q_nR_n &= \hat{Q}_{n-1}^T M_n \hat{Q}_{n-1}, \end{aligned}$$

which we can use to calculate Q_0, R_0, \hat{Q}_0 , then Q_1, R_1, \hat{Q}_1 , then Q_2, R_2, \hat{Q}_2 , and so on.

Due to the sturcture of upper triangular matrices, any product of two upper triangular matrices will have on its diagonal the product of the values on the factors' diagonals⁶. In other words:

⁶ For an upper triangular matrix U , the i -th row will look like this:

$$U_{i,:} = \begin{pmatrix} 0 \\ \vdots \\ 0 \\ U_{i,i} \\ U_{i,i+1} \\ \vdots \\ U_{i,n} \end{pmatrix},$$

while the j -th column will look like this:

$$U_{:,j} = \begin{pmatrix} U_{1,j} \\ \vdots \\ U_{j-1,j} \\ U_{j,j} \\ 0 \\ \vdots \\ 0 \end{pmatrix}.$$

For a product $U = U_1U_2$ the diagonal value $U_{m,m}$ will consist of the dot product between $[U_1]_{m,:}$ and $[U_2]_{:,m}$ which is

$$U_{m,m} = [U_1]_{m,:} \cdot [U_2]_{:,m} = [U_1]_{m,m} [U_2]_{m,m}.$$

$$R_{mm} = \prod_{i=0}^{N-1} [R_i]_{mm}$$

$$\ln(R_{mm}) = \sum_{i=0}^{N-1} \ln([R_i]_{mm}).$$

So to calculate the diagonal values of the final \mathbf{R} , only the diagonal values of each \mathbf{R}_n need to be stored⁷. For the Lyapunov exponents, because the logarithm converts products into sums, we can store just the values of $\ln([R_i]_{mm})$ and average these over time to find an estimate of the exponents:

$$\lambda_m \approx \frac{1}{N\Delta t} \ln(\mathbf{R}_{mm})$$

$$= \sum_{i=0}^{N-1} \frac{1}{N\Delta t} \ln([R_i]_{mm}). \quad (3.3)$$

⁷ Note that, to calculate any \mathbf{R}_n , we need both \mathbf{M}_n and $\hat{\mathbf{Q}}_{n-1}$. Therefore the product of all \mathbf{Q}_n matrices needs to be stored as well.

3.2.4 Implementation of the algorithm

The algorithm as described above has been implemented in Python, using the libraries numpy and scipy for integration, the QR decomposition, and further matrix computations.

The algorithm is largely based on the algorithm in [18]. It is a fairly direct implementation of the equations as described in the previous sections, with the addition of a **decomposition window**. In order to save computation time, we don't have to perform a QR decomposition for every map \mathbf{M}_i , as the main reason for doing this is the numerical instability of calculating the full matrix \mathbf{F} . However, we might be able to calculate the product $\mathbf{M}_{i+L}\mathbf{M}_{i+L-1}\dots\mathbf{M}_{i+1}\mathbf{M}_i$ for a small number of iterations L . This L is our decomposition window, because it specifies how often we perform the QR decomposition.

The main part of the algorithm is specified in code in Appedix A. In order to evaluate the accuracy of the results given by this algorithm, two methods have been developed.

The first of these is the λ^+ -error, or **exponent-sum error**. This is a way to estimate the error in the sum of the exponents for a given system. This is made possible because the sum of the Lyapunov exponents is equal to the average volume expansion, which gives rise to the identity:

$$\lambda^+ = \sum_{i=1}^n \lambda_i = \text{trace}(\mathbf{J}) = \sum_{i=1}^n J_{ii}. \quad (3.4)$$

This means the value of the sum can be calculated in two different ways, and these can be compared. Because the exponents are a time-averaged quantity, we should also calculate the average trace of the Jacobian for systems where the volume expansion is not constant. If the value of the trace is constant, or it converges faster than the Lyapunov exponents

themselves, we can already calculate the sum this way to high accuracy after only a few time steps. Then, comparing the sum of the finite time exponents to the sum given by the trace gives us an error bound of the sum at that point. This tells us about the accuracy of the finite-time Lyapunov exponents with regards to their values in the infinite limit, for which the two sums should be exactly equal. This value then becomes a measure of how far the exponents are along to convergence.

However, having an error value for the sum of the exponents does not tell us anything about the individual values⁸. To give an estimate of the accuracy of the individual values, **convergence plots** have been produced. These plots display how close the value of an exponent is after n time steps, compared to the final value of the exponent. We call this *the distance to the final value*. For example, if the distance seems to be about 10^{-2} near the end of the plot, we cannot be confident in the final value of the exponent up to more than two decimal places. After all, if we had stopped the calculation slightly earlier, its value might have differed by 10^{-2} ! In this way the ‘absolute’ reliability of the actual values for the exponents can be judged from these plots, while the ‘relative’ reliability (have they converged or not) can be judged from the λ^+ -error.

⁸ This is the case because we don’t know if there are correlations between the values. If we know there are none, we could say that

$$(\widetilde{\lambda^+})^2 = \widetilde{\lambda_1}^2 + \dots + \widetilde{\lambda_n}^2 \geq \widetilde{\lambda_i}^2$$

and therefore

$$\widetilde{\lambda_i} \leq \widetilde{\lambda^+}$$

for any $0 \leq i \leq n$ (where $\widetilde{\lambda_i}$ is the error in the i -th exponent). However, we don’t know the correlations are zero, and there are example in which they are most likely not zero.

If we have a time-independent symmetry in the system, it is conservative for example, we expect the values of the Lyapunov exponents to be symmetric as well at any time. This means that, if one exponent grows over time, its symmetric counterpart must grow as well. Therefore there is a clear nonzero correlation between the two.

Results

The results of this project consist of three parts. First, the algorithm for calculating Lyapunov exponents is demonstrated by performing the calculation on the Lorenz system. Then the results for a variety of systems is presented. Afterwards, the behavior of a coupled Nosé-Hoover system is investigated and the relationship between the coupling strength and the Lyapunov spectrum is presented.

4.1 Detailed calculation of the Lyapunov exponents

To illustrate the functioning of the algorithm, one calculation will be discussed in particular. These results are for a calculation on the Lorenz system

$$\dot{\vec{x}} = \begin{pmatrix} \dot{x}_1 \\ \dot{x}_2 \\ \dot{x}_3 \end{pmatrix} = \begin{pmatrix} \sigma(x_2 - x_1) \\ x_1(\rho - x_3) - x_2 \\ x_1x_2 - \beta x_3 \end{pmatrix},$$

with parameters $\sigma = 16$, $\beta = 45.92$ and $\rho = 4$. These parameters were chosen because they are the same as used for the calculation in [18] and so allow for comparison between results.

The further parameters of the algorithm were a trajectory length $T = 3000$ time units, and a time step $\Delta t = 0.04$. Figure 4.1 shows that the region traversed by this trajectory is quite dense, and so it provides a good view of the entire attractor.

The result of the computation of the Lyapunov exponents is given in Figure 4.2, together with a plot of their intermediate values. The values for the λ^+ -error during computation are displayed in Figure 4.3. Finally, the sum of the exponents together with its error are displayed in Figure 4.4.

Because the trace of the Lorenz system is constant, the λ^+ -error only depends on the sum of the exponents. For a system where the mean volume expansion is not constant, the validity of the λ^+ -error should also be

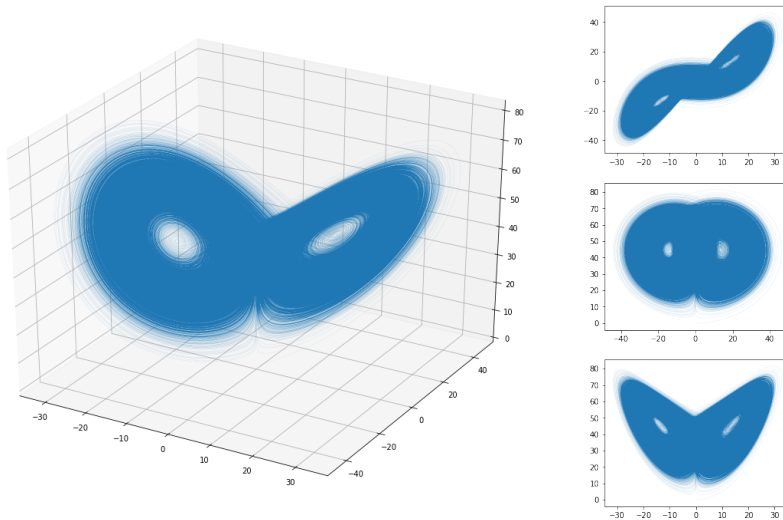


Figure 4.1: A plot of a trajectory of the Lorenz system with parameters $\sigma = 16$, $\beta = 45.92$ and $\rho = 4$, initial conditions $\vec{x}_0 = \begin{pmatrix} 1 \\ 0 \\ 0 \end{pmatrix}$, and a length of 3000 time units. The left plot displays a 3D view, while the right plots display each pair of exponents, with (x, y) from top to bottom: (x_1, x_2) , (x_2, x_3) , (x_1, x_3) .

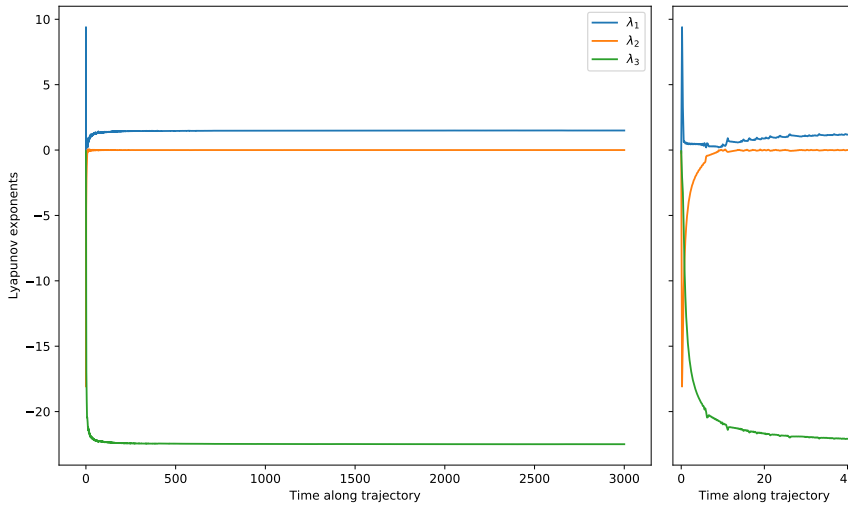


Figure 4.2: The calculation of the Lyapunov exponents for the Lorenz system with parameters $\sigma = 16$, $\beta = 45.92$ and $\rho = 4$. The values at time τ are the finite-time Lyapunov exponents for $t = 0$ to $t = \tau$. The final values at $t = T = 3000$ are: $\lambda_1 = 1.4948$, $\lambda_2 = -0.0001$, $\lambda_3 = -22.4933$, with a sum of $-2.100 \cdot 10^1 \pm 1.4 \cdot 10^{-3}$. The left plot displays the full trajectory, while the right plot displays only the first 40 time units in order to show the speed of convergence more clearly.

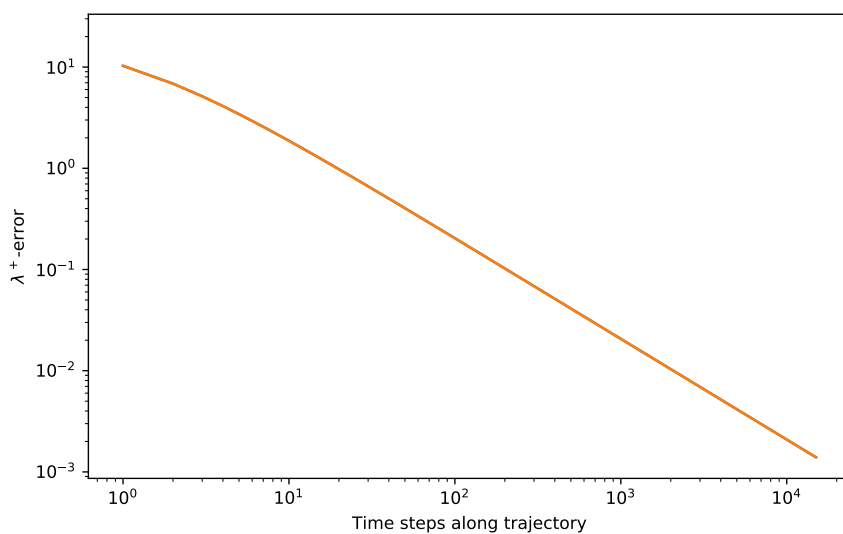


Figure 4.3: A log-log plot of the λ^+ -error for the calculation as in Figure 4.2. This plot is logarithmic to show the λ^+ -error seems to follow a power law. Fitting a function $f(t) = at^k$ gives $a = 19.59$ and $k = -0.9934$.

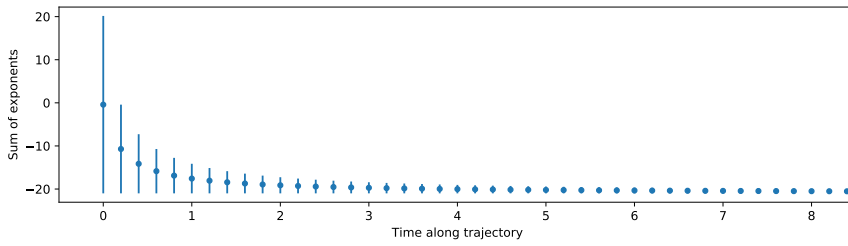


Figure 4.4: The sum of the exponents for the Lorenz system as in Figure 4.2, with the associated error bars given by the λ^+ -error as in Figure 4.3. Only the first 8 time units are shown because the error gets small enough to not be visible anymore after that.

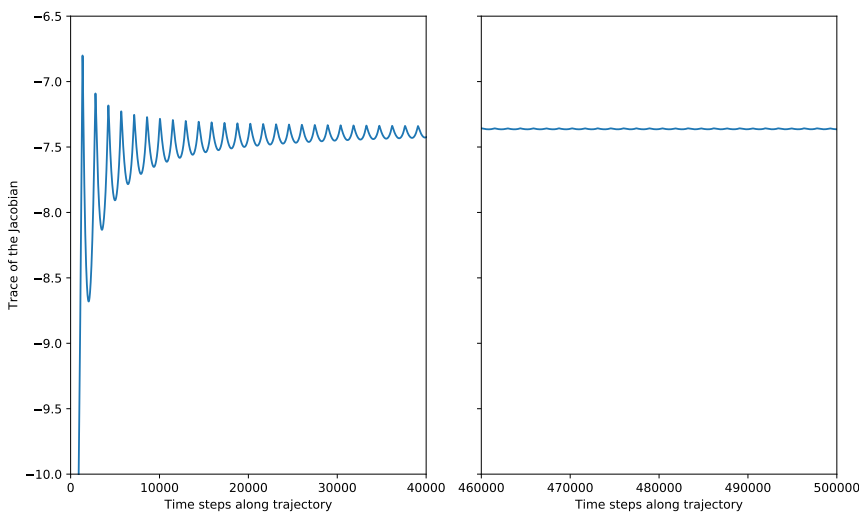


Figure 4.5: The average trace of the Jacobian for the Van der Pol oscillator during a calculation of its Lyapunov exponents. The first and last 40000 steps are plotted. The trace is not constant, but oscillates along the limit cycle. These oscillations dampen over time but don't disappear. The final average value of the trace is -7.364.

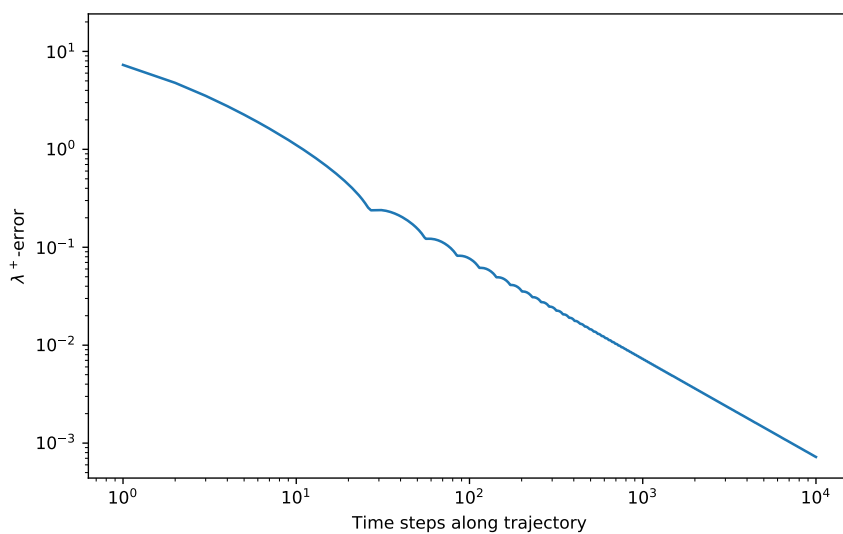


Figure 4.6: A log-log plot of the λ^+ -error for a calculation of the Lyapunov exponents for the Van der Pol oscillator. This plot is logarithmic to show the λ^+ -error seems to follow a power law. Fitting a function $f(t) = at^k$ gives $a = 7.705$ and $k = -1.008$.

tested. For this we take the Van der Pol oscillator,

$$\dot{\vec{x}} = \begin{pmatrix} \dot{x} \\ \dot{v} \end{pmatrix} = \begin{pmatrix} v \\ -x - \mu(x^2 - 1)v \end{pmatrix},$$

with parameter $\mu = 5$. The results for this system can be compared with those from [19]. The Van der Pol oscillator is not chaotic, but a dissipative system with a limit cycle, which should have one zero and one negative exponent. However, its trace is not constant, because there is a friction which depends on x and therefore on time. The trace of the Van der Pol oscillator is shown in Figure 4.5, and the λ^+ -error is shown in Figure 4.6.

4.2 Lyapunov exponents of selected systems

Estimated values of the Lyapunov exponents have also been calculated for a number of other systems. The results are visible in Table 4.1. These systems all fall into one of two categories: they are either a reproduction of earlier calculations for which the results can be checked with the corresponding literature (e.g. the Lorenz system), or they involve one of the systems discussed in Chapter 2.3 that have been selected for numerical investigation.

For each configuration of system and parameters, the iteration time and the final values of the exponents are listed, along with their sum and the associated λ^+ -error. In order to judge the accuracy of the values of the individual exponents and the behavior of the algorithm, convergence plots for all systems have been included in Appendix B. Power-law fits of the λ^+ -errors have also been performed for all the systems and the parameters are listed in Table 4.3. The values for the systems that have been investigated previously are also listed in Table 4.2 for comparison.

These values were calculated using the algorithm implementation as discussed in Chapter 3.2.4. For all calculations, a time step of $\Delta t = 0.04$ has been used, as this appeared to provide sufficiently accurate values for the zero exponents.

Systems that appear in literature are the Lorenz systems (a, b), the Van der Pol oscillators (c, d), the Nosé-Hoover oscillators (e, f), and the driven pendulum (j). Systems that do not appear in the literature but are

System	Parameters	Trajectory length	Exponents	Sum	Reference
(a) Lorenz system 1	$\sigma = 10,$ $\beta = \frac{8}{3},$ $\rho = 10$	3000	$\lambda_1 = 0.8965,$ $\lambda_2 = 0.0006,$ $\lambda_3 = -14.5628$	$-1.367 \cdot 10^1$ $\pm 9.0 \cdot 10^{-4}$	[20]
(b) Lorenz system 2	$\sigma = 16,$ $\beta = 45.92,$ $\rho = 4$	3000	$\lambda_1 = 1.4948,$ $\lambda_2 = -0.0001,$ $\lambda_3 = -22.4933$	$-2.100 \cdot 10^1$ $\pm 1.4 \cdot 10^{-3}$	[18]
(c) Van der Pol oscillator 1	$\mu = 5$	2000	$\lambda_1 = 0.0002,$ $\lambda_2 = -7.3638$	$-7.364 \cdot 10^0$ $\pm 7.2 \cdot 10^{-4}$	[19]
(d) Van der Pol oscillator 2	$\mu = 0.0499922$	2000	$\lambda_1 = 0.0003,$ $\lambda_2 = -0.0490$	$-4.861 \cdot 10^{-2}$ $\pm 4.8 \cdot 10^{-6}$	N/A
(e) Nose-Hoover oscillator 1	$a = 1$	4000	$\lambda_1 = 0.0228,$ $\lambda_2 = -0.0001,$ $\lambda_3 = -0.0219$	$8.082 \cdot 10^{-4}$ $\pm 2.0 \cdot 10^{-8}$	[17]
(f) Nose-Hoover oscillator 2	$a = 3$	4000	$\lambda_1 = 0.0604,$ $\lambda_2 = -0.0000,$ $\lambda_3 = -0.0630$	$-2.609 \cdot 10^{-3}$ $\pm 1.3 \cdot 10^{-7}$	[21]
(g) Coupled harmonic oscillators	$C = 0.05$	2000	$\lambda_1 = -0.0002,$ $\lambda_2 = -0.0002,$ $\lambda_3 = -0.0498,$ $\lambda_4 = -0.0498$	$-9.999 \cdot 10^{-2}$ $\pm 9.8 \cdot 10^{-6}$	N/A
(h) Coupled N-H pair 1	$a = 3,$ $\bar{k} = 1,$ $\Delta k = 0.02,$ $C = 0.034375$	4000	$\lambda_1 = 0.0116,$ $\lambda_2 = 0.0062,$ $\lambda_3 = -0.0025,$ $\lambda_4 = -0.0104,$ $\lambda_5 = -0.0250,$ $\lambda_6 = -0.0358$	$-5.591 \cdot 10^{-2}$ $\pm 2.7 \cdot 10^{-6}$	N/A
(i) Coupled N-H pair 2	$a = 3,$ $\bar{k} = 1,$ $\Delta k = 0.02,$ $C = 0.096875$	4000	$\lambda_1 = 0.0312,$ $\lambda_2 = 0.0051,$ $\lambda_3 = -0.0022,$ $\lambda_4 = -0.0350,$ $\lambda_5 = -0.0606,$ $\lambda_6 = -0.0944$	$-1.559 \cdot 10^{-1}$ $\pm 7.6 \cdot 10^{-6}$	N/A
(j) Driven pendulum	$F = \sin(t)$	4000	$\lambda_1 = 0.1638,$ $\lambda_2 = -0.0000,$ $\lambda_3 = -0.0000,$ $\lambda_4 = -0.1638$	$-8.268 \cdot 10^{-14}$ $\pm 8.3 \cdot 10^{-14}$	[17]
(k) Driven damped pendulum 1	$d_1 = 0.005,$ $F = \sin(t)$	2000	$\lambda_1 = 0.0088,$ $\lambda_2 = -0.0000,$ $\lambda_3 = -0.0000,$ $\lambda_4 = -0.0588$	$-5.000 \cdot 10^{-2}$ $\pm 4.9 \cdot 10^{-6}$	N/A
(l) Driven damped pendulum 2	$d_2 = 0.005,$ $F = e^{-0.0025t} \sin(t)$	2000	$\lambda_1 = 0.0325,$ $\lambda_2 = -0.0025,$ $\lambda_3 = -0.0025,$ $\lambda_4 = -0.0325$	$-5.000 \cdot 10^{-3}$ $\pm 4.9 \cdot 10^{-7}$	N/A
(m) Pendulum driven by Van der Pol oscillator	$\mu = 0.0499922$	4000	$\lambda_1 = 0.1879,$ $\lambda_2 = 0.0002,$ $\lambda_3 = -0.0495,$ $\lambda_4 = -0.1879$	$-4.930 \cdot 10^{-2}$ $\pm 2.4 \cdot 10^{-6}$	N/A

Table 4.1: The estimated Lyapunov exponents for a variety of systems. (a) and (b) are instances of the Lorenz system, which are well researched in literature. (c) and (d) are not chaotic, but dissipative systems with a limit cycle. (e) and (f) are Nosé-Hoover (NH) oscillators, where both configurations also appear in the literature. (g) is an example of the coupling introduced in section 2.3.2. (h) and (i) are examples of coupled NH oscillators, where one is more weakly and one more strongly coupled. (j) is a configuration of the (4D) driven pendulum which shows chaotic behavior, and (k) and (l) are identical but with an added damping. In (m) the pendulum is instead driven by a Van der Pol oscillator as in (d).

System	Reference	Exponents	Reference exponents	Sum	Reference sum
Lorenz system 1	[20]	$\lambda_1 = 0.8965,$ $\lambda_2 = 0.0006,$ $\lambda_3 = -14.5628$	$\lambda_1 = 0.90563,$ $\lambda_2 = 0,$ $\lambda_3 = -14.57219$	$-1.367 \cdot 10^1$ $\pm 9.0 \cdot 10^{-4}$	$-1.366 \cdot 10^1$
Lorenz system 2	[18]	$\lambda_1 = 1.4948,$ $\lambda_2 = -0.0001,$ $\lambda_3 = -22.4933$	$\lambda_1 = 1.4978,$ $\lambda_2 = -0.0037,$ $\lambda_3 = -22.4940$	$-2.100 \cdot 10^1$ $\pm 1.4 \cdot 10^{-3}$	$-2.099 \cdot 10^1$
Van der Pol oscillator 1	[19]	$\lambda_2 = -7.3638$	$\lambda_2 = -7.362$	$-7.364 \cdot 10^0$ $\pm 7.2 \cdot 10^{-4}$	N/A
Nosé-Hoover oscillator 1	[17]	$\lambda_1 = 0.0228$	$\lambda_1 = 0.0139$	$8.082 \cdot 10^{-4}$ $\pm 2.0 \cdot 10^{-8}$	N/A
Nosé-Hoover oscillator 2	[21]	$\lambda_1 = 0.0604$	$\lambda_1 = 0.061 \pm 0.001$	$-2.609 \cdot 10^{-3}$ $\pm 1.3 \cdot 10^{-7}$	N/A

Table 4.2: The values of Lyapunov exponents for a number of systems together with reference values from literature. When a value is omitted (or N/A) this is because it is not mentioned or not all exponents are calculated so the sum can not be calculated either.

System	k	a	Behavior w.r.t. volumes
Lorenz system 1	-0.9968	13.0396	Dissipative
Lorenz system 2	-0.9934	19.5894	Dissipative
Van der Pol oscillator 1	-1.0077	7.7048	Dissipative
Van der Pol oscillator 2	-0.7064	0.0037	Dissipative
Nose-Hoover oscillator 1	-1.9946	11.6745	Conservative
Nose-Hoover oscillator 2	-1.9978	50.4616	Conservative
Coupled harmonic oscillators	-0.9966	0.0952	Dissipative
Coupled N-H pair 1	-1.3397	1.2234	Dissipative
Coupled N-H pair 2	-1.1471	0.5086	Dissipative
Driven pendulum	0.1513	0.0000	Conservative
Driven damped pendulum 1	-0.9966	0.0476	Dissipative
Driven damped pendulum 2	-0.9966	0.0048	Dissipative
Pendulum driven by Van der Pol oscillator	-0.7991	0.0074	Dissipative

Table 4.3: The parameters for a power law fit $f(t) = at^k$ for the λ^+ -error of the calculations in Table 4.1. The average of k for all the dissipative systems is $\langle k \rangle = 0.998$.

motivated in this thesis are the coupled harmonic oscillators (g):

$$\dot{\vec{x}} = \begin{pmatrix} \dot{x}_1 \\ \dot{v}_1 \\ \dot{x}_2 \\ \dot{v}_2 \end{pmatrix} \quad (4.1)$$

$$\dot{x}_{1,2} = v_{1,2}$$

$$\dot{v}_{1,2} = -x_{1,2} - C(v_{1,2} - v_{2,1}) - \frac{C^2}{2}(x_{1,2} - x_{2,1}),$$

the coupled N-H pairs (h, i):

$$\dot{\vec{x}} = \begin{pmatrix} \dot{x}_1 \\ \dot{v}_1 \\ \dot{s}_1 \\ \dot{x}_2 \\ \dot{v}_2 \\ \dot{s}_2 \end{pmatrix} \quad (4.2)$$

$$\dot{x}_{1,2} = v_{1,2}$$

$$\dot{v}_{1,2} = -k_{1,2}x_{1,2} - v_{1,2}s_{1,2} - C(v_{1,2} - v_{2,1}) - \frac{C^2}{2}(x_{1,2} - x_{2,1})$$

$$\dot{s}_{1,2} = a(v_{1,2}^2 - 1),$$

where $k_{1,2} = \bar{k} \pm \Delta k$, the damped driven pendulums (k, l):

$$\dot{\vec{x}} = \begin{pmatrix} \dot{\phi}_1 \\ \dot{\omega}_1 \\ \dot{\phi}_2 \\ \dot{\omega}_2 \end{pmatrix} = \begin{pmatrix} \omega_1 \\ \phi_2 - \sin(\phi_1) - d_1\omega_1 \\ \omega_2 \\ -\phi_2 - d_2\omega_2 \end{pmatrix}, \quad (4.3)$$

and the pendulum driven by a Van der Pol oscillator (m):

$$\dot{\vec{x}} = \begin{pmatrix} \dot{\phi} \\ \dot{\omega} \\ \dot{x} \\ \dot{v} \end{pmatrix} = \begin{pmatrix} \omega \\ x - \sin(\phi) \\ v \\ -x - \mu(x^2 - 1)v \end{pmatrix}. \quad (4.4)$$

4.3 Coupled Nosé-Hoover oscillators

Values of the Lyapunov exponents were calculated for a specific configuration of coupled Nosé-Hoover oscillators, while varying parameter C which indicates the strength of the coupling. In total calculations were performed for $2^5 + 1$ equally spaced values of the coupling parameter C between 0 and 0.1. The results are visible in Figure 4.7. The other parameters where $a = 3$, $\bar{k} = 1$, and $\Delta k = 0.02$, were a is chosen in order to

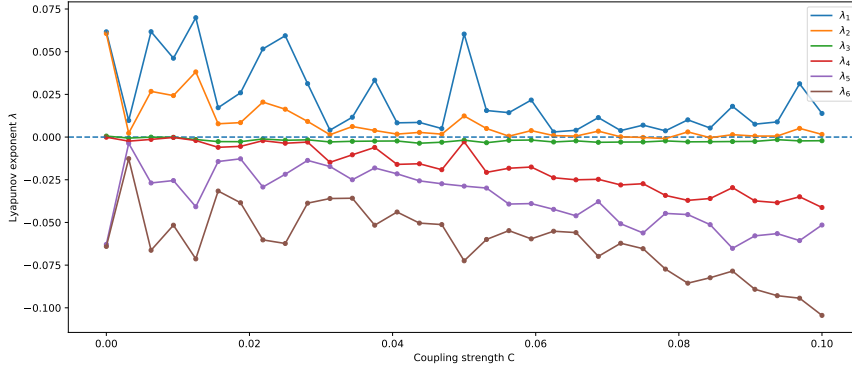


Figure 4.7: A plot of the Lyapunov exponents of instances of two coupled Nosé-Hoover oscillators as in Eq. 4.2 for $2^5 + 1$ equally spaced values of the coupling parameter C between 0 and 0.1. The value 0 on the y-axis is indicated by a blue dashed line to separate the positive, negative and (approximately) zero exponents. The other parameters that were chosen are $a = 3$, $\bar{k} = 1$, and $\Delta k = 0.02$, and the trajectory length is 4000 time units.

maximize the chaotic behavior, and Δk is nonzero so that the coupled oscillators are slightly dissimilar, as in [12]. The trajectory length used was 4000 time units, as longer trajectories would take too much in the calculations, and none of the other systems have problems converging before that time.

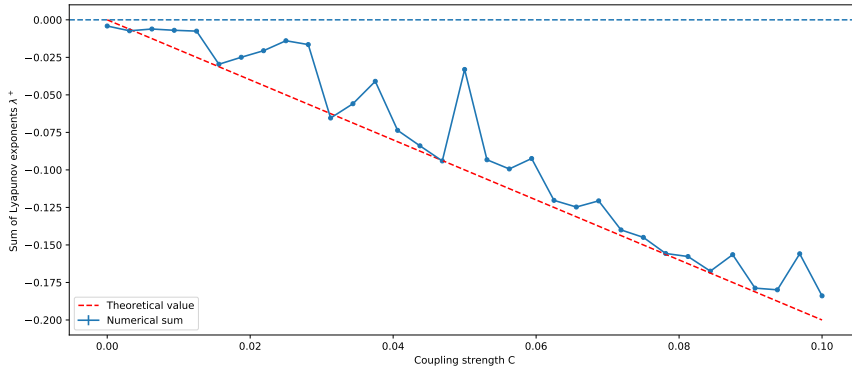


Figure 4.8: A plot of the sum of the Lyapunov exponents of the coupled Nosé-Hoover oscillators in Figure 4.7. The blue line indicates sums of the numerical exponents, while the red dashed line shows the theoretically expected value of $\lambda^+ = \text{trace}(\mathbf{J}) = -2C$. The λ^+ -errors are also plotted but too small to be visible. The value 0 on the y-axis is indicated by a light blue dashed line.

The sum of the Lyapunov exponents for these coupled oscillators is displayed in Figure 4.8. Also displayed is the theoretical value of the sum, which is:

$$\lambda^+ = \langle \text{trace}(\mathbf{J}) \rangle = \left\langle \frac{\partial v_1}{\partial v_1} + \frac{\partial v_2}{\partial v_2} \right\rangle = 2 \cdot -C. \quad (4.5)$$

Discussion

5.1 Accuracy of the calculations

The Lyapunov spectrum algorithm gives satisfactory results. For a system like the Lorenz system, the values seem to converge rather quickly: after only 50 time units the overall shape of the spectrum is already visible. For all systems, the final sum error is quite small: the relative error is almost always on the order of 10^{-4} , which means the sum is correct up to three digits.

In comparison with the literature, the Lorenz system also fares reasonably well: the values of the calculated exponents and their sums and those from the references differ by 10^{-2} at most. For the other systems, the results are similarly accurate, except for the first configuration of the Nosé-Hoover (NH) oscillator, which was compared with the book by Sprott [17]. Here the values are noticeably different (their relative difference is about 0.6), though their absolute difference is still on the order of 10^{-2} . However, the results for the other configuration of the N-H oscillator (compared with the article by Posch et. al. [21]) are more accurate, with the maximal exponent differing by about 10^{-3} absolutely and 10^{-2} relatively.

It should be noted that the numerical values of the exponents for the N-H oscillator are quite small in magnitude and not very stable during the calculation (as shown by the corresponding convergence plot). It might be the case that the matching values from Posch et. al. [21] are more accurate (as they use about 10^7 time steps) than the values from Sprott, for which the trajectory length used is not mentioned. Otherwise it could be possible that the N-H oscillator with $a = 1$ actually doesn't have chaotic but quasiperiodic behavior, and the positive and negative exponents go to zero in the infinite-time limit, but take very long to do so in practice.

The sum error seems to be a well-behaved measure: for the Lorenz

system as well as the Van der Pol oscillator it seems to follow a power law. In the case of the Van der Pol oscillator, the oscillations in the trace are visible in the error as well, but the overall relationship still seems valid, especially over a long calculation. In both cases assuming a power law

$$\lambda^+(t) = at^k$$

gives an exponent of $k \approx -1$. This means the error scales approximately as $\frac{1}{t}$, which means making a calculation twice as long will make the sum error twice as small. Therefore a longer calculation than the ones performed will not have a significant effect on the sum error.

In the case of the Lorenz system (b), this relationship means after 50 time units we expect the sum error to be about

$$\lambda^+(T) \cdot \frac{T}{t} = 1.4 \cdot 10^{-3} \cdot \frac{3000}{50} = 8.4 \cdot 10^{-2},$$

i.e. a relative error of $4 \cdot 10^{-3}$. This is in agreement with the observation that the spectrum has visibly converged after that time, and equally agrees with the values from the literature as the final values do. This indicates that after these first 50 time units the spectrum has ‘practically’ converged, in that the results are unlikely to converge to a value that is more accurate for any practical purpose, as a slightly different method of calculating the values might provide different results. Thus a good **stopping condition**, i.e. way to check when the calculation is sufficiently accurate and the results can be accepted, might be to check when the λ^+ -error is smaller than 10^2 .

The time to achieve this convergence differs per system, as it is also determined by the constant a in the power law fit. However, this value seems to be related to the average trace of the Jacobian, as for the Lorenz system $a = 19.59$ and for the Van der Pol oscillator $a = 7.705$, which in both cases is on the same order as the final value of λ^+ . As this can be calculated quite easily (often analytically and otherwise numerically with quick convergence) the trajectory length needed in order to estimate the Lyapunov exponents sufficiently well can be estimated beforehand as:

$$\lambda^+(t) = at^k \approx \frac{|\text{trace}(\mathbf{J})|}{t} \leq \epsilon$$

$$t \geq \frac{|\text{trace}(\mathbf{J})|}{\epsilon}, \tag{5.1}$$

where ϵ is the **tolerance**, or desired accuracy, so in this example $\epsilon = 10^{-2}$. However, this relationship does not apply (as noted) for conservative systems where $\text{trace}(\mathbf{J}) \approx 0$. This is shown in Table 4.3, where for the conservative systems either $a = 0$ or a has a seemingly arbitrary, large

¹ Note that, as mentioned before, the sum-error might not indicate convergence at all for systems with a certain symmetry. This has been observed in Hamiltonian systems such as the driven pendulum, where the sum error is always very small ($\approx 10^{-14}$). This follows from this relationship, because when $\lambda^+ \approx 0$, $a \approx 0$ (see Table 4.3), and the power law time dependence $\lambda^+ \propto t^{-1}$ is invalid.

value².

A zero exponent clearly appears for all the systems: there is always one exponent whose absolute value is smaller than 10^{-3} , except in the coupled N-H pairs (which are the most complicated systems investigated) and in one of the damped driven pendulums. Moreover, in each system which is expected to show a certain symmetry, the symmetry is clearly visible, excepting the Nosé-Hoover oscillators.

This shows that the Nosé-Hoover oscillators, while appearing simple from their definition, are in fact tougher to simulate and evaluate correctly than the other systems. Also, while there can be much variability in their behavior, their Lyapunov exponents remain small, as the configuration (f) is the most chaotic configuration known for a single oscillator [21]. Nonetheless the (positive) Lyapunov exponents remain smaller than 10^{-1} , which makes it difficult to distinguish the zero exponent and makes it harder to calculate the values accurately.

5.2 Coupling the Nosé-Hoover oscillators

The effect of coupling two Nosé-Hoover oscillators as in Eq. 4.2 is shown in Figure 4.7. Starting at $C = 0$, the full spectrum is simply the union of the two 3D spectra, which are themselves very similar. Then, as the coupling increases, it is apparent that there is no simple relationship between the coupling strength C and the Lyapunov spectrum. Some values are ‘unlucky’ and the exponents are smaller in magnitude, indicated they show less chaotic and more periodic behavior, while some, even large values of C are lucky and retain the chaotic behavior.

Two main trends can be spotted in Figure 4.7. First off, the negative exponents get progressively more negative as C increases. This is because of the effective damping that occurs when coupling oscillators: namely the damping of the velocity difference $C(v_{1,2} - v_{2,1})$. Additionally, the systems start off with two (approximately) zero exponents, λ_3 and λ_4 , which over time split into one zero and one negative exponent. This shows how a spectrum with a (+, +, 0, -, -, -) signature can be formed from two systems with a (+, 0, -) signature: the effective damping causes the zero exponents to split and the line of symmetry to fall below zero.

However, the small magnitude of the exponents makes it hard to distinguish the cases where there are two approximately zero exponents from those where one of the two is negative. Later on, the same happens when the originally positive λ_2 nears zero. Only in a few lucky cases the distinction that there is a (+, +, 0, -, -, -) signature can be made, of which two were included in Table 4.1 as examples: one where the zero exponents just start to split, and one where C is close to 0.1 and yet the positive

² The difference is most likely that the driven pendulum is instantaneously conservative while the N-H oscillators are periodically conservative, and thus the sum error does shrink over time but there is no clear power law relationship.

exponents are relatively large in magnitude.

Looking at the sum in Figure 4.8 shows the trend that would be expected, that it grows in the negative direction proportional to C . However, there are fluctuations, which indicates the behavior of the coupling is not as simple as expected: it is not the only thing affecting the average volume contraction. What might be happening here is that the interaction with the ‘heat bath’ s is causing side-effects. After all, the velocities have a non-constant friction $-s_{1,2}v_{1,2}$ in addition to the coupling, so the sum of the exponents is dependent on $s_{1,2}$ as well. The full equation for the sum is:

$$\lambda^+ = \langle \text{trace}(J) \rangle = -2C - \langle s_1 \rangle - \langle s_2 \rangle. \quad (5.2)$$

In the uncoupled case $\langle s_{1,2} \rangle$ are equal to zero, leading to a sum proportional to C . However, in the coupled case s_1 and s_2 are also indirectly coupled through the velocities, which could produce a different result. In Figure 4.8 the relation (5.2) above is shown to be correct, as adding the averages of $s_{1,2}$ retrieves the proportional relationship:

$$\lambda^+ + \langle s_1 \rangle + \langle s_2 \rangle = -2C - \langle s_1 \rangle - \langle s_2 \rangle + \langle s_1 \rangle + \langle s_2 \rangle = -2C. \quad (5.3)$$

5.2.1 Symmetry of the coupled spectrum

We have already seen that the nonzero average value of $s_{1,2}$ leads to a friction which affects the volume expansion and thus the Lyapunov exponents. For the sum this is visible in Figure 4.8 as when adding the average values of $s_{1,2}$ the result is nearly equal to $-2C$. Another question to ask is: is the spectrum still symmetric around a negative value? This was one of the objectives we were aiming for when choosing to couple two conservative oscillators.

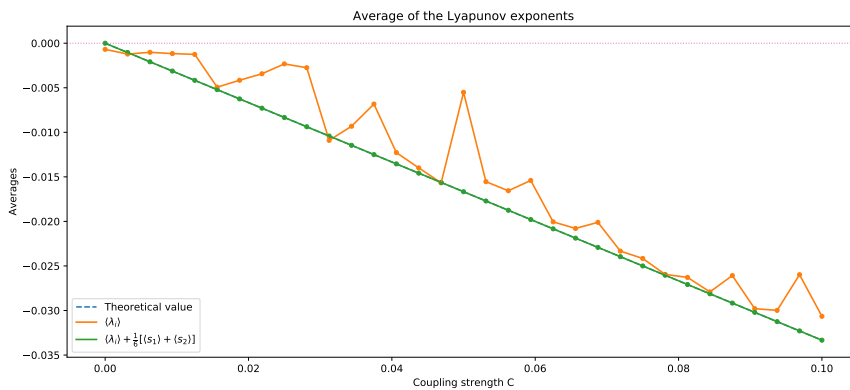


Figure 5.1: The average of the Lyapunov exponents for the coupled Nosé-Hoover oscillators, whose spectra are shown in Figure 4.7. The numerical average is plotted and compared with the theoretically expected value $\langle \lambda_i \rangle = -\frac{C}{3}$, where it is assumed that $\langle s_{1,2} \rangle = 0$. Subtracting the average value of $s_{1,2}$ from the average of the exponents, gives a value that agrees with the expected value.

If the spectrum of Lyapunov exponents is symmetric, it must be symmetric around its average value. Therefore it makes sense to calculate the

average. Because the average is related to the sum, it follows that

$$\langle \lambda_i \rangle = \frac{\lambda_1 + \lambda_2 + \lambda_3 + \lambda_4 + \lambda_5 + \lambda_6}{6} = \frac{\lambda^+}{6} = -\frac{C}{3} - \frac{1}{6}[\langle s_1 \rangle + \langle s_2 \rangle], \quad (5.4)$$

so it is equal to $-\frac{C}{3}$ when the average of $s_{1,2}$ is zero. This can also be motivated from the system specification: a uniformly damped system will have a spectrum symmetric around the value

$$-\frac{\gamma}{2},$$

where γ is the damping coefficient. In the case of the coupled N-H oscillators, we have two coupled harmonic oscillators, each damped with coefficient C , and the two thermostats which are undamped. In other words, out of the 6 equations, 4 of them are damped with coefficient C while 2 are undamped. Therefore it can be argued that the ‘effective’ uniform damping on the system is:

$$\gamma_{\text{eff}} = \frac{4}{6}C = \frac{2}{3}C.$$

From this, it also follows that the spectrum should be symmetric around a value

$$-\frac{\gamma_{\text{eff}}}{2} = -\frac{C}{3}.$$

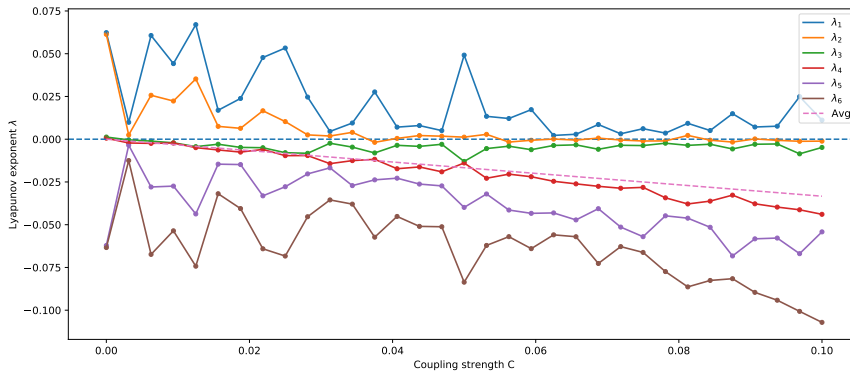


Figure 5.2: A shifted version of the spectra of coupled Nosé-Hoover oscillators as in Figure 4.7. The spectra are shifted proportionally to the respective value of $\langle s_{1,2} \rangle$, so that the average of the exponents agrees with the theoretical value (a straight line, as indicated in the plot).

For illustration purposes, in Figure 5.2, the spectra have been shifted up by

$$\frac{1}{6}[\langle s_1 \rangle + \langle s_2 \rangle],$$

so that their average is equal to $-\frac{C}{3}$, which is indicated in the plot by a red dashed line. Here it can already be seen that the spectrum is not symmetric, even when factoring out the average influence of $\langle s_{1,2} \rangle$, as λ_3 is much further from the average line than λ_4 . The asymmetry of the spectrum is also clearly visible in Figure 5.3, where the exponents have been shifted so that their average is zero, and the last 3 exponents have changed sign. If the spectrum were symmetric, the pairs of exponents

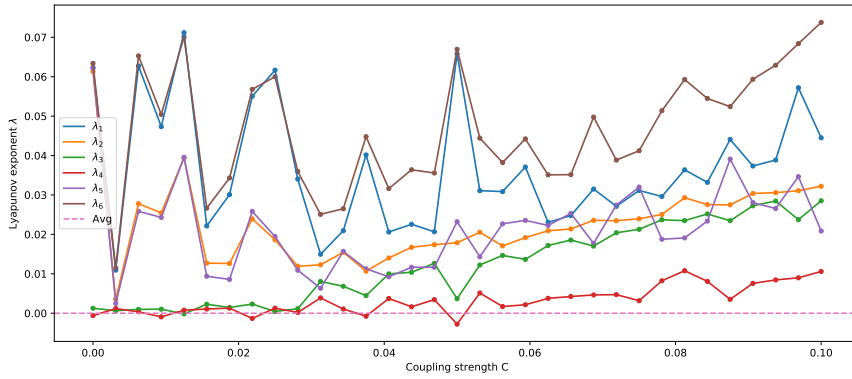


Figure 5.3: A visual check of the possible symmetry in the spectra of coupled Nosé-Hoover oscillators as in Figure 4.7. The exponents have been shifted so that their average is equal to zero, i.e. so that the line in Figure 5.2 corresponding to the average ends up at zero. Then the exponents below the average have been flipped around the symmetry axis. If the spectrum is symmetric, the pairs of exponents $(\lambda_{1,2,3}, \lambda_{6,5,4})$ should coincide.

should overlap. It can be seen that for small C this is somewhat the case, but for larger C they deviate. From this it can be concluded that the coupling of the two oscillators does not just have an unexpected effect on the net volume expansion, it also breaks the symmetry of the Lyapunov spectrum.

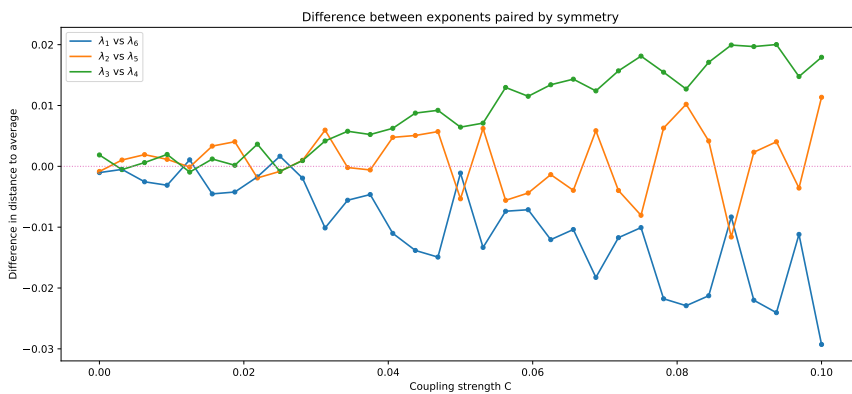


Figure 5.4: The differences between the pairs of exponents in Figure 5.3. Their sum is zero (by definition), and a positive value means the pair is shifted in the positive direction (i.e. the largest exponent is relatively further from the symmetry axis), while a negative value means the opposite (i.e. the largest exponent is relatively closer to the symmetry axis).

Finally, in Figure 5.4 the differences between the symmetric pairs of exponents are displayed, in order to show how the asymmetry is reflected in the values of the exponents. On average, three trends are visible:

- The pair (λ_1, λ_6) has a mostly negative difference, which means that λ_6 is relatively further from the symmetry axis than λ_1 .
- The pair (λ_2, λ_5) has an average difference around zero, which means that λ_2 and λ_5 are approximately symmetric.
- The pair (λ_3, λ_4) has a mostly positive difference, which means that λ_4 is relatively closer to the symmetry axis than λ_3 .

This gives us a good qualitative view of the asymmetry of the Lyapunov spectra, as shown in Figure 5.5. The exponents above the symmetry line move closer together, while the exponents below move further apart.

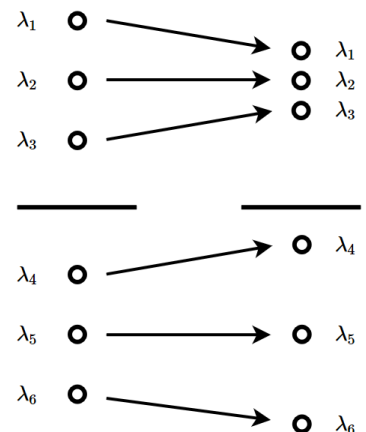


Figure 5.5: A schematic view of the asymmetry in the spectrum of coupled Nosé-Hoover oscillators. The left part of the image shows a symmetric spectrum, while the right part shows a typical spectrum for this system. The exponents above the symmetry line move closer together, while the exponents below move further apart.

distinguish and to calculate accurately. Also, it tells us that the asymmetry is mostly reflected in the exponents largest in magnitude and those smallest in magnitude.

5.3 The (damped) driven pendulum

For the driven pendulum, the configuration (j) which is also featured in [17] shows clear chaotic behavior with a positive exponent of $1.638 \cdot 10^{-1}$, and a $(+, 0, 0, -)$ signature. Also, the spectrum is symmetric around zero, which makes clear that it is conservative, and it has been calculated very accurately: the sum error 10^{-14} could even be called suspiciously small. Because this system is conservative, the sum error is probably not very meaningful, but from the convergence plot Figure B.10 in Appendix B the individual exponents seem to be converging properly as well.

In order to see whether a system with a $(+, 0, -, -)$ signature could also be found (this being a 4D analog to the *C. elegans* spectrum), a number of ways to introduce a negative exponent were investigated. Applying a damping term to either the pendulum or the driving harmonic oscillator seems to destroy the chaotic behavior of the system. When damping the driving oscillator, this makes sense: even slightly damping it will cause the driving force to go to zero, after which the pendulum will fall back into periodic motion, and so the chaotic behavior persists only for a limited time.

When damping the pendulum, this seems less apparent. The most likely reason is that the main property of the pendulum (which distinguishes it qualitatively from a harmonic oscillator) is that it has the ability to ‘swing over the top’, i.e. make a full revolution without passing through $\phi = 0$, and the damping makes this kind of motion unlikely if the driving force does not compensate for it. This then makes the chaotic behavior disappear. Also, the damping of the pendulum only seems to make the most negative exponent more negative, and doesn’t introduce another negative exponent, which makes sense, because the driving oscillator is still conservative and thus still contributes two dimensions in which the volume scaling is zero.

This makes clear that the driving oscillator should be dissipative in some way. One configuration that has been tested is replacing the harmonic oscillator with a Van der Pol oscillator, which in fact does introduce a negative exponent belonging to the VdP oscillator, but also shows chaotic behavior, with an even larger positive exponent than the conservative case. This is most likely because the Van der Pol oscillator has a limit cycle around radius $r = 2$, leading to a driving force with two times the amplitude of $F = \sin(t)$.

5.4 Similarity to the *C. elegans* Lyapunov spectrum

From the results obtained we can evaluate whether models have been found that show a Lyapunov spectrum similar to *C. elegans*. The *C. elegans* spectrum is characterised by the appearance of the $(+, +, 0, -, -, -)$ signature for the signs of the exponents, and a clear symmetry in the values of the exponents.

This signature could be replicated clearly in the case of the driven pendulum. The driving of the normally $(0,0)$ signed pendulum changes its spectrum into a $(+,-)$ signed one, so that the total system has a $(+,0,0,-)$ signature. The driving oscillator can then be made dissipative in some way, so that one of its exponents becomes negative, leading to a $(+,0,-,-)$ spectrum.

The upside of this configuration is that the effect of the driving is clear and isolated in the two exponents that belong to the pendulum's motion, so that the change in the spectrum is predictable. However, the symmetry is not maintained, as the driving is unidirectional, which means there cannot be a global symmetry as the pendulum's exponents do not affect the 'driving exponents'. Thus, if the exponents for the pendulum are $(\lambda_1, \lambda_4) = (a, -a)$, the driving oscillator should be adjusted to be $(\lambda_2, \lambda_3) = (0, -b)$, with b chosen so that the full spectrum is symmetric. However, if the spectrum is symmetric around a value $-S$, this symmetry means that

$$\lambda_1 + S = -(\lambda_4 + S) \tag{5.5}$$

$$\lambda_2 + S = -(\lambda_3 + S) \tag{5.6}$$

$$\lambda_1 + S - (\lambda_2 + S) = \lambda_1 - \lambda_2 \tag{5.7}$$

$$= a - 0 = a \tag{5.8}$$

$$= -(\lambda_4 + S) + (\lambda_3 + S) \tag{5.9}$$

$$= \lambda_3 - \lambda_4 \tag{5.10}$$

$$= -b + a = a - b, \tag{5.11}$$

and so $a = a - b$ and $b = 0 = \lambda_3$, which means that for this configuration we cannot have both a symmetric spectrum and a $(+,0,-,-)$ signature.

For the coupled Nosé-Hoover oscillators, the difficulties are more complicated. First of all, the symmetry is not conserved after coupling. This occurs because the two thermostats s_1 and s_2 'interfere', causing the exponents to deviate from the symmetric shape. However, a different way of coupling the equations that takes into account the presence of these extra thermostat variables, might be able to conserve the symmetry. For example, this could be attempted by writing the full system in a Hamiltonian

formulation and applying the same reasoning as in Section 2.1.6 in order to derive theoretically symmetry-conserving coupled equations.

Nonetheless, even if a symmetry-conserving coupling is possible, there is much variation in the Lyapunov spectrum that makes it hard to say this system is a natural fit for a $(+, +, 0, -, -, -)$ signed spectrum. This is because there are two opposing effects at work: the coupling constrains the motion of the system³, leading to a net dissipation, which splits the two zero exponents into a $(0, -)$ pair, leading to the right signature. However, if the coupling is too strong this dissipation will dampen the already weak chaotic behavior, which might make one of the positive exponents go to zero or below, leading to a $(+, 0, 0, -, -, -)$ or $(+, 0, -, -, -)$ signature. In this sense the signature of the *C. elegans* spectrum does not naturally emerge from the coupling of these systems, and while it is possible, it is also very sensitive to the parameters of the system.

However, what is particularly clear is that this system is much more complex than meets the eye. More research could be done into how the thermostats interact, and how the spectrum could be coupled in a more stable way. Also, if the source of the chaotic behavior (like the pendulum going over the top), maybe it could get clearer how to couple them in a way that constrains them but does not destroy the chaotic component.

Finally, if a configuration of this system is obtained that clearly has the right spectrum, it might be interesting to investigate what the behavior looks like in phase space compared to *C. elegans*' dynamics: is the motion mostly regular with occasional 'chaotic events', comparable to *C. elegans* moving forward pseudo-sinusoidally and suddenly turning? Or is the behavior always slightly aperiodic but globally unvarying? The ability to pose these kind of questions shows that the behavior of this system still contains plenty of possibilities for further research.

³ This has also been sighted in preliminary calculations (not included here) of the attractor (Kaplan-Yorke) dimension of the coupled Nosé-Hoover system, which shows the dimension erratically decreasing from 6 to 3 as coupling is increased.

Conclusion

In order to analyse the behavior of the worm and model organism *C. elegans* from a physical perspective, data about its crawling movements has been collected and analyses on it have been performed previously [1]. The objective of this project has been to investigate a number of dynamical systems with origins motivated in physics or elsewhere, in order to see whether their dynamics might resemble the dynamics of the *C. elegans* locomotive system that has been reconstructed from data.

The metric by which it is determined if these dynamics resemble each other is the Lyapunov spectrum¹, which gives the average expansion of volumes in phase space under the dynamics. From this spectrum, a few properties of the system can be determined, most notably its energy dissipation and whether it has a (semi-)Hamiltonian structure. The *C. elegans* has been shown to have a symmetric, dissipative spectrum, which indicates it has a Hamiltonian structure with uniform damping applied.

The systems chosen to investigate were a pair of coupled Nosé-Hoover (N-H) oscillators, and a driven pendulum. The N-H oscillators are conservative by themselves, and it has been shown that coupling them induces a net dissipation. However, the effect on the whole spectrum is hard to predict, as the symmetry is not conserved. This means the effective damping applied by the coupling is not uniform and should be adjusted.

The driven pendulum shows very predictable results. Applying a periodic driving force makes the spectrum of the pendulum non-zero but symmetric around zero, which means it obtains chaotic behavior. The rest of the spectrum is determined by the spectrum of the driving oscillator. However, it is not possible to construct a fully symmetric spectrum in this way while having a net damping, and so this system cannot be compared to the dynamics of *C. elegans* in its current form.

In summary, the driven pendulum shows a too limited range of behavior in order to show dynamics resembling those of *C. elegans*, and has to be extended in some way. The coupled N-H oscillators, however, show a

¹ In other words, the set of all Lyapunov exponents for a system.

wide range of behavior which indicates they might be useful if coupled in a different way. The first objective in such an attempt would be to find a way of coupling them so that the net dissipation is only caused by the coupling².

Further research could also be done on the behavior of the coupled N-H oscillators: what do the dynamics look like in phase space compared to those of *C. elegans*? Additionally, an alternative to the (harmonically) driven pendulum is the double pendulum, which could not be properly investigated in this project due to technical difficulties with the system. Further analysis might be performed to see whether the double pendulum could also produce a qualitatively similar Lyapunov spectrum.

² Right now, a part of the dissipation is caused by the two thermostats interfering, which leads to unpredictable behavior.

Bibliography

- [1] Tosif Ahamed and Greg Stephens. C.elegans locomotion is governed by a 6d quasi-Hamiltonian chaotic attractor. 2016.
- [2] John G White, Eileen Southgate, J Nichol Thomson, and Sydney Brenner. The structure of the nervous system of the nematode *Caenorhabditis elegans*. *Philos Trans R Soc Lond B Biol Sci*, 314(1165):1–340, 1986.
- [3] RA Kosinski and M Zaremba. Dynamics of the model of the *Caenorhabditis Elegans* neural network. *Acta Physica Polonica B*, 38:2201, 2007.
- [4] Greg J Stephens, Bethany Johnson-Kerner, William Bialek, and William S Ryu. Dimensionality and dynamics in the behavior of c. elegans. *PLoS Comput Biol*, 4(4):e1000028, 2008.
- [5] Andre EX Brown and Benjamin de Bivort. Ethology as a physical science. *bioRxiv*, 2018.
- [6] Steven H. Strogatz. *Nonlinear Dynamics And Chaos: With Applications To Physics, Biology, Chemistry, And Engineering (Studies in Nonlinearity)*. Westview Press, 2001.
- [7] Holger Kantz and Thomas Schreiber. *Nonlinear Time Series Analysis*. Cambridge University Press, 2004.
- [8] J-P Eckmann and David Ruelle. Ergodic theory of chaos and strange attractors. *Reviews of Modern Physics*, 57(3):617, 1985.
- [9] Ute Dressler. Symmetry property of the Lyapunov spectra of a class of dissipative dynamical systems with viscous damping. *Physical Review A*, 38(4):2103, 1988.
- [10] André E Botha and Guoyuan Qi. Analysis of the triple pendulum as a hyperchaotic system.

- [11] André E Botha and Guoyuan Qi. Optimised periodic and hyperchaotic modes of a triple pendulum.
- [12] Michael G Rosenblum, Arkady S Pikovsky, and Jürgen Kurths. Phase synchronization of chaotic oscillators. *Physical Review Letters*, 76(11):1804, 1996.
- [13] Tirth Shah, Rohitashwa Chattopadhyay, Kedar Vaidya, and Sagar Chakraborty. Conservative perturbation theory for nonconservative systems. *Phys. Rev. E*, 92:062927, Dec 2015.
- [14] CP Dettmann and GP Morriss. Hamiltonian reformulation and pairing of Lyapunov exponents for Nosé-Hoover dynamics. *Physical Review E*, 55(3):3693, 1997.
- [15] William G Hoover. Remark on “Some simple chaotic flows”. *Physical Review E*, 51(1):759, 1995.
- [16] Ikuo Fukuda. Coupled Nosé–Hoover lattice: A set of the Nosé–Hoover equations with different temperatures. *Physics Letters A*, 380(33):2465–2474, 2016.
- [17] Julien C Sprott. *Elegant chaos: algebraically simple chaotic flows*. World Scientific, 2010.
- [18] Z-M Chen, K Djidjeli, and WG Price. Computing lyapunov exponents based on the solution expression of the variational system. *Applied Mathematics and Computation*, 174(2):982–996, 2006.
- [19] Johan Grasman, Ferdinand Verhulst, and Shagi-Di Shih. The lyapunov exponents of the van der pol oscillator. *Mathematical methods in the applied sciences*, 28(10):1131–1139, 2005.
- [20] Julien Clinton Sprott and Julien C Sprott. *Chaos and time-series analysis*, volume 69. Citeseer, 2003.
- [21] Harald A Posch, William G Hoover, and Franz J Vesely. Canonical dynamics of the nosé oscillator: Stability, order, and chaos. *Physical review A*, 33(6):4253, 1986.

Partial code for the Lyapunov exponents algorithm

Below is the main part of the code for the Lyapunov exponent algorithm as discussed in Section 3.2.4. Dots indicate a part of the code has been removed for clarity.

```
1 def le_system_trajectory(sys, tr, dt, L=50, ...):
2     f, Df = sys
3     # Number of points in the trajectory.
4     N = tr.shape[0]
5     # Total number of decompositions.
6     M = int(np.floor((N - 1) / L)) + 1
7     # The dimension of the phase space (excluding t).
8     dim = tr.shape[1] - 1
9
10    # Use a n-parallelepiped as starting volume.
11    V = np.identity(dim)
12    # Keep track of the total sequence of Q's.
13    Qhat = np.identity(dim)
14    # Store the current average exponents in a vector.
15    LE = np.zeros((dim,))
16    ...
17    for i in range(N):
18        # Extract the phase-space point.
19        s, t = ...
20        # Calculate flow map (takes point 1 timestep ahead, linearly).
21        J = Df(t, s)
22        M = expm(dt * J, order=4) # np.identity(dim) + dt * J + mpow(dt * J, 2)/2
23                                # + mpow(dt * J, 3)/6 + mpow(dt * J, 4)/24
```

```

24 # Apply flow to volume.
25 V = np.dot(M, V)
26 ...
27 # Calculate exponents every L steps.
28 if i % L == 0:
29     # 'Realign' the volume matrix to the previously stretched axes.
30     V = multi_dot([Qhat.T, V, Qhat])
31     # Separate into rotation (Q) and stretching/shearing (R) transformation.
32     Q, R = qr_pos(V)
33     # Calculate "instantaneous" exponents as the logarithm
34     # of the diagonal of R.
35     Rdl = np.log(np.diag(R)) / L
36     # Add the instantaneous exponents to the current moving average
37     # over the trajectory.
38     m = int(i / L)
39     LE = LE + (Rdl - LE)/(m + 1)
40     ...
41     # Save the total orthonormal basis for the next iteration.
42     Qhat = np.dot(Qhat, Q)
43     # Reset the volume to an identity volume.
44     V = np.identity(dim)
45
46 # Average the exponents over time, i.e. samples (already done) * timestep.
47 LE = LE / dt
48 # Sort them for convenience.
49 sorted = np.argsort(LE)[::-1]
50 LE = LE[sorted]
51 ...
52 return LE

```

APPENDIX B

Convergence plots

This appendix contains convergence plots for the Lyapunov exponent calculations for all the systems in Table 4.1. These plots show for each exponent the difference between its value after n time steps along the trajectory and its final value, after the algorithm has completed. The distance to the final value is plotted logarithmically on the y-axis, and is simply the absolute difference between the current and final value:

$$|\lambda_i(n) - \lambda_i(N)|.$$

Here N is the trajectory length given by $N = \frac{T}{\Delta t}$, where T is the trajectory length (from Table 4.1) and $\Delta t = 0.04$. The rapid falloff at the end of the plots should be ignored, as the distance to the final value can get arbitrarily close to 0 near the end of the run and so this does not tell us anything about the accuracy of the value of the exponent.

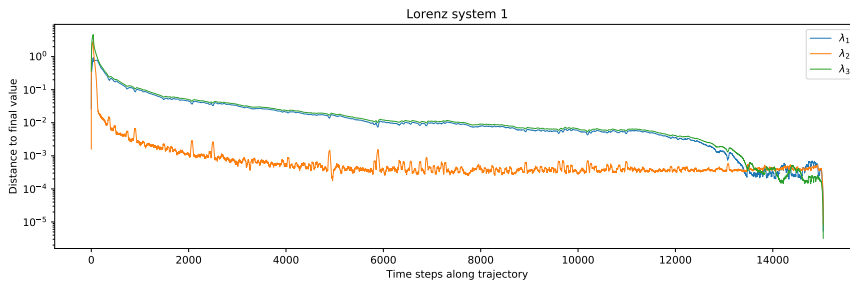


Figure B.1: The convergence plot for system *Lorenz system 1* with parameters $\sigma = 10$, $\beta = \frac{8}{3}$, $\rho = 10$.

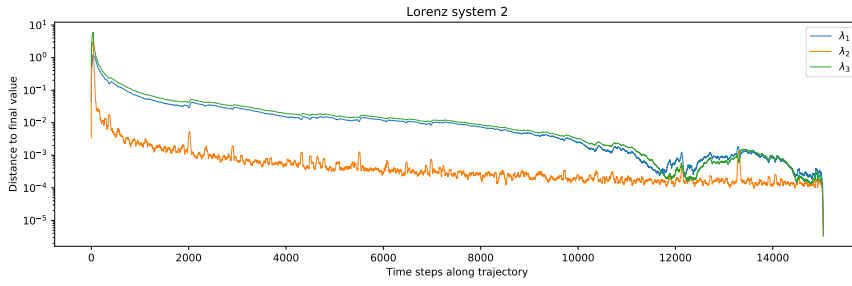


Figure B.2: The convergence plot for system *Lorenz system 2* with parameters $\sigma = 16$, $\beta = 45.92$, $\rho = 4$.

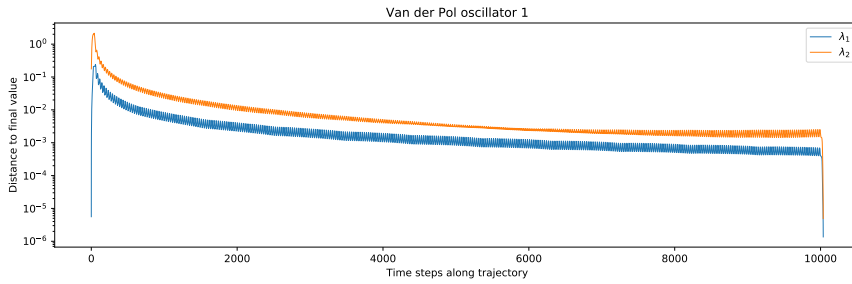


Figure B.3: The convergence plot for system *Van der Pol oscillator 1* with parameters $\mu = 5$.

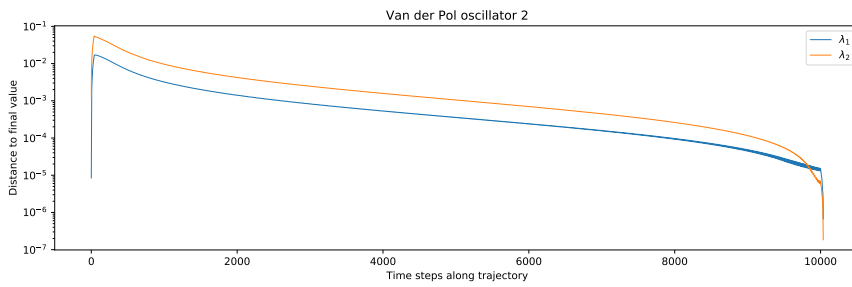


Figure B.4: The convergence plot for system *Van der Pol oscillator 2* with parameters $\mu = 0.0499922$.

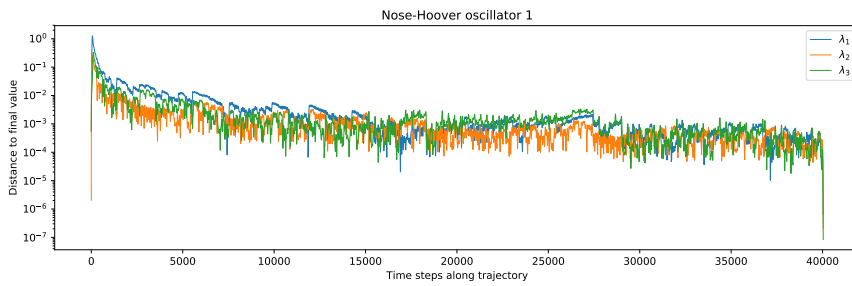


Figure B.5: The convergence plot for system *Nose-Hoover oscillator 1* with parameters $a = 1$.

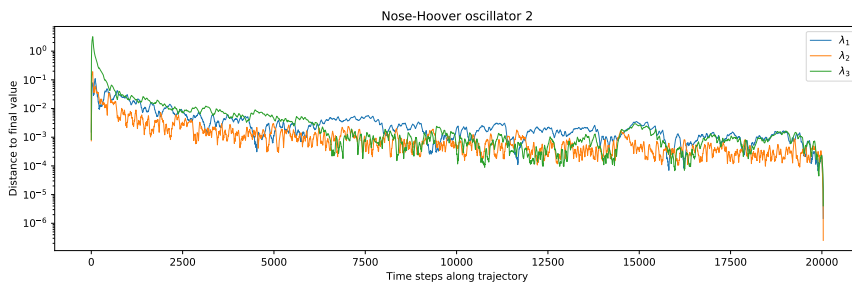


Figure B.6: The convergence plot for system *Nose-Hoover oscillator 2* with parameters $a = 3$.

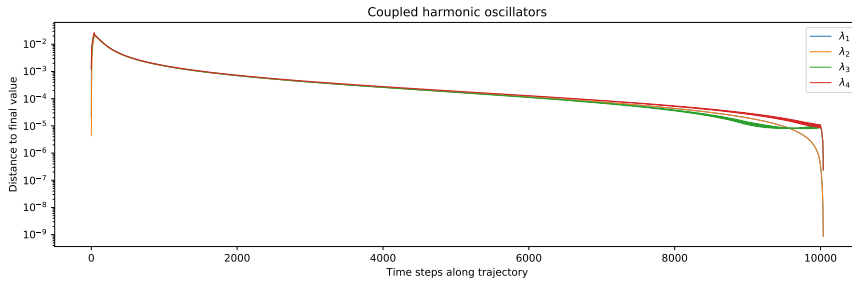


Figure B.7: The convergence plot for system *Coupled harmonic oscillators* with parameters $C = 0.05$.

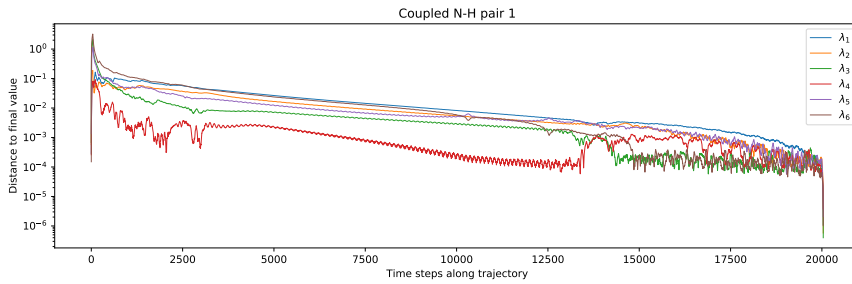


Figure B.8: The convergence plot for system *Coupled N-H pair 1* with parameters $a = 3, \bar{k} = 1, \Delta k = 0.02, C = 0.034375$.

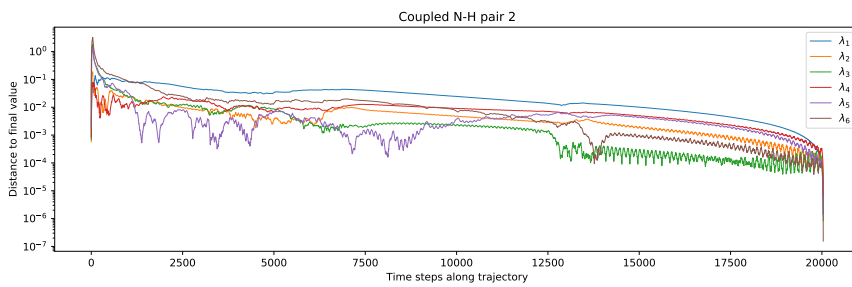


Figure B.9: The convergence plot for system *Coupled N-H pair 2* with parameters $a = 3, \bar{k} = 1, \Delta k = 0.02, C = 0.096875$.

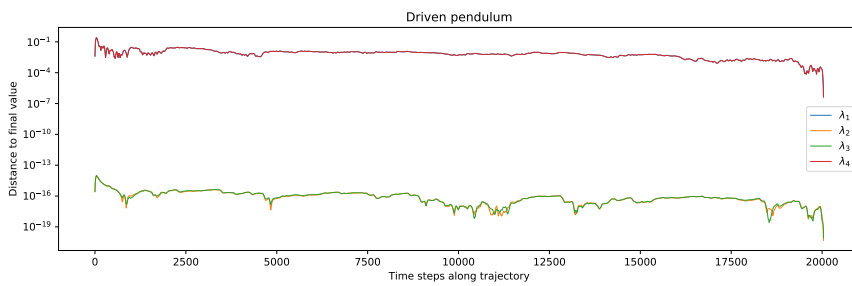


Figure B.10: The convergence plot for system *Driven pendulum* with parameters $F = \sin(t)$.

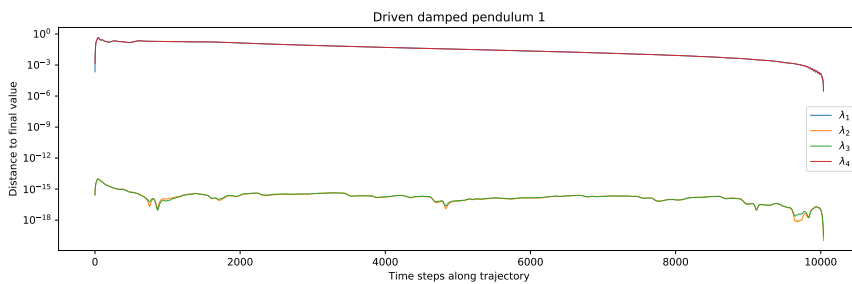


Figure B.11: The convergence plot for system *Driven damped pendulum 1* with parameters $d_1 = 0.005, F = \sin(t)$.

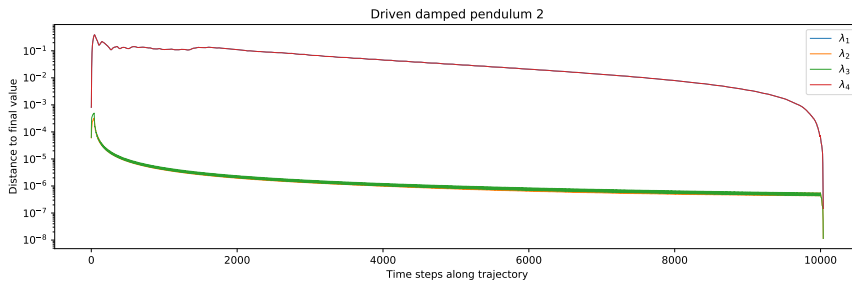


Figure B.12: The convergence plot for system *Driven damped pendulum 2* with parameters $d_2 = 0.005$, $F = e^{-0.0025t} \sin(t)$.

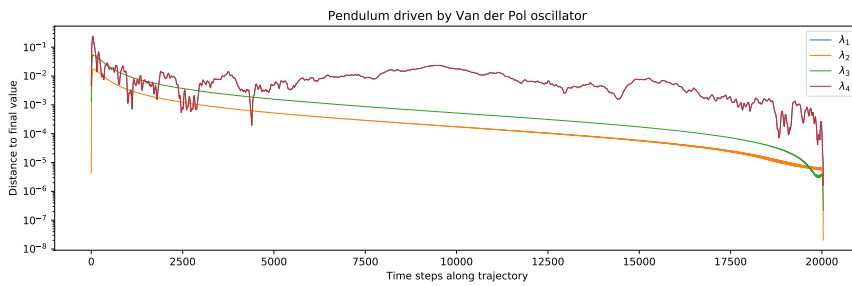


Figure B.13: The convergence plot for system *Pendulum driven by Van der Pol oscillator* with parameters $\mu = 0.0499922$.